ONLINE FIRST

This is a provisional PDF only. Copyedited and fully formatted versión will be made available at final publication

HISTOLOGY AND HISTOPATHOLOGY

ISSN: 0213-3911
e-ISSN: 1699-5848

Lonp1 expression and correlation with mitophagy and immune infiltration markers in colon adenocarcinoma

Authors: Giada Zanini, Valentina Selleri, Giorgia Sinigaglia, Giulia Micheloni, Isabella Martusciello, Stefania Caramaschi, Milena Nasi, Luca Reggiani Bonetti and Marcello Pinti

DOI: 10.14670/HH-25-037
Article type: ORIGINAL ARTICLE
Accepted: 2026-01-13
Epub ahead of print: 2026-01-22

Lonp1 expression and correlation with mitophagy and immune infiltration markers in colon adenocarcinoma

Giada Zanini[1], Valentina Selleri[1,2], Giorgia Sinigaglia[1], Giulia Micheloni[1], Isabella Martusciello[1]

Stefania Caramaschi[3], Milena Nasi[3], Luca Reggiani Bonetti[4], Marcello Pinti[1,2*]

[1] Department of Life Sciences, University of Modena and Reggio Emilia, 41125 Modena, Italy.

[2] National Institute for Cardiovascular Research – INRC, 40126 Bologna, Italy.

[3] Department of Surgical, Medical, Dental and Morphological Sciences, University of Modena and Reggio Emilia, 41125 Modena, Italy.

[4] Department of Medical and Surgical Sciences for Children and Adults, University of Modena and Reggio Emilia, 41125 Modena, Italy.

[*] Correspondence: marcello.pinti@unimore.it Tel.: +39052055386

Keywords: Lon protease; colorectal cancer; mitochondrial turnover; tumor-infiltrating lymphocytes.

Short title: Lonp1 in colon adenocarcinoma

Abstract

LONP1, a mitochondrial ATP-dependent protease, plays a crucial role in mitochondrial homeostasis by regulating protein turnover and mitophagy. Recent studies have highlighted its upregulation in various cancers, including colorectal cancer (CRC). This study investigates the expression of LONP1 in colon adenocarcinoma (COAD) and its correlation with mitophagy-related proteins and immune infiltration markers. Using publicly available databases and immunohistochemical analysis of 50 COAD patient samples, we confirmed that LONP1 expression is significantly elevated in COAD compared with normal tissue. High LONP1 levels were associated with tumor progression, TP53 mutation status, and poor prognosis. Correlation analyses revealed that LONP1 is closely linked to mitochondrial dynamics, mitophagy regulators (PINK1, AMBRA1, FUNDC1), and metabolic reprogramming. Additionally, LONP1 expression positively correlated with tumor-infiltrating lymphocytes, particularly CD8+ T cells, suggesting a potential role in immune evasion. Immunohistochemical analysis distinguished two patterns: high LONP1/low TOMM20 expression associated with aggressive tumors and low LONP1/high TOMM20 expression linked to better outcomes and stronger immune infiltration. These findings suggest that LONP1 contributes to tumor progression through mitochondrial regulation and immune modulation, highlighting its potential as both a prognostic biomarker and a therapeutic target in COAD.

1. Introduction

LONP1, also known as Lon protease 1, is a highly conserved ATP-dependent protease located in the mitochondrial matrix, where it plays a crucial role in maintaining mitochondrial proteostasis and overall cellular homeostasis. LONP1 selectively degrades misfolded, oxidatively damaged, or surplus mitochondrial proteins, thereby ensuring the integrity of mitochondrial proteins under both normal and stress conditions. LONP1 exerts several functions in the cells (Gibellini *et al.*, 2020). In particular, LONP1 binds to and regulates mitochondrial DNA (mtDNA) and is involved in maintaining mtDNA stability, influencing mitochondrial gene expression. LONP1 participates in metabolic regulation by modulating key enzymes involved in the tricarboxylic acid (TCA) cycle and oxidative phosphorylation (OXPHOS). LONP1 expression is upregulated under various stress conditions, including oxidative stress, hypoxia, and proteotoxic stress. It protects mitochondrial functionality by degrading damaged proteins and maintaining proper folding of stress-sensitive mitochondrial enzymes, such as heat shock proteins (Gibellini *et al.*, 2022). For instance, oxidative stress induces LONP1 via nuclear factor erythroid 2-related factor 2 (NRF2) and NF-κB pathways, while LONP1 overexpression amplifies reactive oxygen species (ROS) production, thereby promoting tumorigenic Ras-MEK-ERK signaling (Pinti *et al.*, 2011; Cheng *et al.*, 2013). Hypoxia further induces LONP1 expression through hypoxia-inducible factor (HIF)-1α and HIF-2α, facilitating cancer cell survival under low oxygen conditions (Di *et al.*, 2016).

LONP1 contributes to mitophagy, the selective autophagic degradation of damaged mitochondria. It plays a role in regulating key components of mitophagy pathways, such as phosphatase and tensin homologue (PTEN)-induced putative kinase 1 (PINK1). The PINK1-Parkin pathway relies on ubiquitination to tag damaged mitochondria for degradation. PINK1 accumulates on mitochondria with low membrane potential, phosphorylates ubiquitin, and activates Parkin, which further ubiquitinates outer mitochondrial membrane (OMM) proteins. This cascade recruits autophagy adapters, like sequestosome-1 (p62/SQSTM1), nuclear domain 10 protein 52 (NDP52), and Optineurin (OPTN), linking ubiquitinated mitochondria to autophagosomes (Lazarou *et al.*, 2015; Yoo and Jung, 2018). LONP1 supports this process by degrading PINK1 under normal conditions; its depletion leads to PINK1 accumulation, highlighting the role of LONP1 in mitochondrial maintenance. Moreover, the PINK1/Parkin pathway is closely interconnected with molecules and pathways involved in mitochondrial dynamics, such as mitofusin 1 (MFN1) and MFN2, responsible for mitochondrial fusion. MFN1 and MFN2 are highly susceptible to ubiquitination by Parkin. MFN2 promotes the recruitment of Parkin to damaged mitochondria, and PINK1 phosphorylates MFN2, enhancing its ubiquitination by Parkin (Tanaka *et al.*, 2010). Consequently, PINK1/Parkin activation leads to rapid ubiquitination and degradation of MFN1 and MFN2, preventing fusion between damaged and healthy mitochondria (Tanaka *et al.*, 2010).

Proteins such as FUN14 domain-containing 1 (FUNDC1), BCL2-interacting protein 3 (BNIP3), and NIP3-like protein X (NIX) interact directly with autophagy-related proteins (ATGs) via LC3-interacting regions (LIRs). Under hypoxia, FUNDC1 undergoes dephosphorylation, enhancing its interaction with LC3 and promoting mitophagy (Liu *et al.*,

2012). LONP1 stabilizes mitochondrial dynamics through interactions with FUNDC1, as its depletion leads to mitochondrial defects, reduced ATP production, and increased ROS levels. Reconstitution of LONP1 in FUNDC1-deficient cells restores mitochondrial function and reduces cancer cell motility and invasion (Li *et al.*, 2020).

Several studies highlighted the upregulation of LONP1 as a typical feature of various cancers, including colorectal cancer, melanoma, glioblastoma, and bladder cancer. LONP1-haploinsufficient mice exhibit higher resistance to tumorigenesis, suggesting its critical role in cancer progression (Bernstein *et al.*, 2012; Cheng *et al.*, 2013; Nie *et al.*, 2013; Liu *et al.*, 2014; Quiros *et al.*, 2014; Di *et al.*, 2016; Gibellini *et al.*, 2018).

The metabolic reprogramming characteristic of cancer cells, such as alterations in OXPHOS and glycolysis, is influenced by LONP1. It regulates enzymes like succinate dehydrogenase subunit B (SDHB) and E1α and supports epithelial-to-mesenchymal transition (EMT), a key step in cancer metastasis. LONP1 enhances EMT markers (N-cadherin, Snail) and stabilizes β-catenin by modulating Akt and GSK-3β pathways (Gibellini *et al.*, 2018). LONP1 is also involved in proneural-mesenchymal transition, particularly in glioblastomas harboring IDH mutations, demonstrating its role in aggressive cancer phenotypes.

This study aims to investigate the expression levels of LONP1 in colon adenocarcinoma (COAD) and its correlation with mitophagy-related proteins and immune infiltration markers. By analyzing publicly available datasets and performing immunohistochemical (IHC) analysis on COAD patient samples, we seek to determine the role of LONP1 in tumor progression, mitochondrial regulation, and immune response. Our findings may provide insights into LONP1 as a potential prognostic biomarker and therapeutic target in colorectal cancer.

2. Materials and Methods

2.1 Clinical specimens

Fifty cases of COAD were selected from the archives of the Pathology Department at the Azienda Ospedaliero-Universitaria Policlinico di Modena. The study was approved by the local Ethics Committee (Prot CE-AVEN N°1103/2021, SIRER ID 3711, Ref. Prot. 15590; May 25, 2021). Patient sex, age at diagnosis, tumor location within the colon, tumor size, and macroscopic/endoscopic appearance were extracted from medical records. Histological examination included all original tissue sections stained with hematoxylin and eosin, evaluated under optical microscopy. The following histomorphological features were recorded: i) Microscopic growth pattern (expansive or infiltrative); ii) Histological subtype and differentiation grade; iii) Tumor aggressiveness features (Lokuhetty *et al.*), including lymphovascular invasion, tumor budding, perineural invasion, intratumoral lymphocytosis; and iv) Pathological tumor stage based on the TNM system (Edge *et al.*, 2010).

2.2 Immunohistochemistry

The most representative paraffin-embedded block of the tumor and peritumoral stroma was selected for analysis. Sections of 4 μm thickness were cut and mounted on positively charged slides for IHC staining. Slides were dried overnight at 40°C to enhance tissue adhesion. The sections were processed using the BENCHMARK ULTRA IHC/ISH ROCHE automated immunostainer (Roche Diagnostics, Basilea, Switzerland), following the datasheet protocols for various markers. The instrument automatically carried out the following steps: i) Deparaffinization and rehydration; ii) Antigen retrieval (CC1-induced) for 36 minutes at 95°; iii) Blocking endogenous peroxidases with hydrogen peroxide; iv) Incubation with selected antibodies at 37°C as per the selected protocol; and v) Reaction development using the Ventana ultraView Universal DAB Detection Kit, employing an avidin-biotin peroxidase complex (ABC) system with diaminobenzidine (DAB) as the chromogenic substrate, and counterstaining with hematoxylin. Antigen expression was visually represented by a brown chromogenic precipitation distinct from the blue hematoxylin counterstaining. Positive control tissues were included to validate the staining reactions. Specifically, the immunohistochemical expression of the following proteins was investigated: LONP1 (Primm), TOMM20 (Santa Cruz Biotechnology, #sc-17764), MFN2 (Abgent, #RB21136), CD3-CD4-CD8 (Leica Biosystems, Deer Park, IL, USA, #HI01A-005), E-Cadherin (Cohesion Biosciences, #CPA1198), N-Cadherin (Cohesion Biosciences, #CPA1200), Vimentin (Cohesion Biosciences, #CPA1198), TWIST (Cloud-Clone, #PAC838Hu01), SIRT3 (Santa Cruz Biotechnology, #sc-365175), SNAIL (ABclonal Technology, #A5243), and PINK1 (Cloud-Clone, #PAL057Hu01).

2.3 Evaluation of IHC staining

Evaluation of IHC staining was performed using a double-blind control procedure: two pathologists evaluated and scored all tissue specimens. For immunohistochemical analysis, a semi-quantitative score was used in combination with the percentage of positive area and the intensity of the staining. LONP1 staining intensity score (negative=0, weak=1, moderate=2, strong=3). We defined markers immunostaining values 0-2 as normal expression and 3 as overexpression.

2.4 Analysis of publicly available datasets

The following public databases have been inspected for LONP1 expression in different types of tumors, and for the analysis of correlation with mitophagy proteins, and immune cells infiltrate:

- Tumor Immune Estimation Resource (TIMER) (https://cistrome.shinyapps.io/timer/): this web-based platform facilitates comprehensive analysis of tumor-infiltrating immune cells. The TIMER database was utilized to investigate the expression patterns of LONP1 mRNA in both cancerous and non-cancerous tissues. The "DiffExp module" was employed to compare LONP1 expression levels between tumor and normal tissues within The Cancer

Genome Atlas (TCGA) dataset. Additionally, the "SCNA module" was used to evaluate the association between tumor infiltration levels and different copy number variations (CNVs) of LONP1 (Li *et al.*, 2017). The "Correlation module" was applied to assess the relationship between LONP1 expression and immune marker genes in COAD, while the "Survival module" was used to examine the association between immune cell infiltration and clinical outcomes.

- GEPIA2 database (http://gepia2.cancer-pku.cn/): GEPIA2 is an upgraded web server for gene expression profiling and interactive analyses in cancer and normal tissues (Tang *et al.*, 2019). The database was utilized to analyze LONP1 expression across multiple malignancies. Additionally, LONP1 expression levels were specifically evaluated in normal colon tissue and CRC.

- UALCAN database (https://ualcan.path.uab.edu/): the "TCGA module" of the UALCAN database was employed to compare LONP1 mRNA expression levels in tumor versus normal tissues. In this study, we evaluated LONP1 expression in COAD while accounting for TP53 mutational status.

- LinkedOmics Database (http://www.linkedomics.org/): this database is a comprehensive collection of multiomics and clinical data from 32 cancer types, including 11,158 patient profiles from TCGA. The "Correlation module" was employed to investigate the relationship between LONP1 expression and immune marker genes in COAD, while the "SCNA module" was used to analyze immune cell infiltration in relation to LONP1 CNVs. Furthermore, the “Link Interpreter module’s Gene Set Enrichment Analysis (GSEA)” was used to explore the biological processes associated with the *LONP1* gene. The GSEA analysis was conducted using the following criteria: the false discovery rate (FDR) was determined based on Rank Criteria from the LinkFinder results; the minimum gene set size was set to three; and a total of 500 permutations were performed.

- Kaplan-Meier Plotter (https://kmplot.com/analysis/index.php?p=home): this online tool is used to analyze the prognostic value of LONP1. The patient samples are split into two groups and compared using a Kaplan-Meier survival plot, and the hazard ratio with 95% confidence intervals and logrank *P* value are calculated (Gyorffy, 2024).

2.5 Cell culture

A human colon carcinoma cell line, SW620 (ATCC), was used in this study. Cells were maintained in Glutamax RPMI 1640 medium supplemented with gentamycin and 10% fetal bovine serum (FBS; Life Technologies, Carlsbad, CA, USA). Cells were cultured in a standard incubator at 37°C and 5% CO_2 in a humidified atmosphere. When specified, to induce mitophagy, cells were treated with 10 μM carbonyl cyanide m-chlorophenyl hydrazone (CCCP) for six hours.

2.6 Cell transfection and retroviral transduction

The pMSCV-Puro empty vector and the pMSCV containing cDNA encoding for the full-length isoform of LONP1 tagged at C-term with enhanced green fluorescent protein (eGFP) (pMSCV-Lon-ISO1-eGFP), were used to transiently transfect the amphotrophic Phoenix (phxA) cell line. The transfection was carried out using Lipofectamine 3000 (Life Technologies, Carlsbad, CA, USA) along with 20 µg of every single plasmid and 0.9 µg of a helper plasmid. The retroviral supernatants generated from the transfection were used for stable transfection of SW620 cells, which were then selected and maintained in medium supplemented with 2 µg/mL puromycin.

2.7 RNA interference

Reverse transfection of cells was performed using RNAiMAX (Thermo Fisher Scientific, Waltham, MA, USA) and 100 nM of three pre-validated siRNA (s17901, s17902, and s17903, Thermo Fisher Scientific) targeting Lonp1 mRNA. Following a 72-hour incubation period, the cells were collected.

2.8 Western blotting

Cell lysates were prepared using RIPA lysis buffer supplemented with protease and phosphatase inhibitor cocktails (Sigma-Aldrich, St. Louis, MO, USA). Proteins were separated by SDS-PAGE (sodium dodecyl sulfate–polyacrylamide gel electrophoresis) on precast gels (8%; Thermo Fisher Scientific) and transferred to nitrocellulose membranes (Bio-Rad Laboratories) for immunoblotting. To optimize the hybridization process, the membranes were cut prior to incubation with primary antibodies. Primary antibodies used included anti-LONP1 (Primm), anti-PINK1 (Cloud-Clone, #PAL057Hu01), and anti-βactin (Abcam, Cambridge, UK, #ab8227). Secondary antibodies were HRP-conjugated goat anti-rabbit and horseradish peroxidase (HRP)-conjugated goat anti-mouse (Bio-Rad Laboratories; #1706515, #1706516). Protein detection was performed using Enhanced Clarity chemiluminescent substrate (Bio-Rad Laboratories) and visualized with a ChemiDoc MP system (Bio-Rad Laboratories). Image analysis was carried out using Image Lab software version 5.2.1.

2.9 Immunofluorescence and confocal microscopy

Cells were cultured on coverslips in 24-well plates and then fixed with 3.7% formaldehyde in PBS (Sigma-Aldrich) for 9 minutes, followed by acetone fixation at −20 °C for 5 minutes (Sigma-Aldrich) and permeabilization with 0.1% Triton X-100 in PBS for 6 minutes (Sigma-Aldrich). After blocking with 3% bovine serum albumin (BSA) for 30 minutes, cells were incubated for one hour at room temperature with primary antibodies against LONP1 (Primm), mitochondria (anti-hMIT, Sigma-Aldrich #MAB1273), and PINK1 (Cloud-Clone, #PAL057Hu01), each diluted 1:100 in 3% BSA. Following washes, Alexa Fluor–conjugated

secondary antibodies (Alexa Fluor® 488 Goat anti-Mouse, #A-11017; Alexa Fluor® 647 Goat anti-Rabbit, #A-21246; Life Technologies) were applied at a 1:200 dilution for one hour at room temperature in 3% BSA, and unbound antibodies were removed by washing. Nuclei were counterstained with 4′,6-diamidino-2-phenylindole (DAPI; 0.5 µg/mL), and coverslips were mounted with Fluoromount (Sigma-Aldrich). Images were acquired using an SP8-AOBS confocal microscope (Leica Microsystems, Wetzlar, Germany) and analyzed with ImageJ and ScanR software.

2.10 RNA extraction and quantitative real-time PCR

Total RNA was isolated from cells using the Quick-RNA Miniprep Plus Kit (Zymo Research, Irvine, CA, USA) according to the manufacturer's protocol. The elution was performed in 100 µL of DNase/RNase-free water. The RNA concentration was measured using a NanoDrop ND-1000 spectrophotometer (Thermo Fisher Scientific). Subsequently, 1 µg of RNA was subjected to reverse transcription using the iScript cDNA synthesis kit (Bio-Rad). Relative expression levels of the genes *LONP1*, *PINK1*, and *TOMM20* were measured by quantitative real-time PCR, using a set of pre-validated wet-lab oligos from Bio-Rad. Real-time PCR was carried out in triplicate using the SsoAdvanced Universal SYBR Green Supermix (Bio-Rad), following the recommended reaction setup and thermal cycling conditions, in a CFX96 Touch instrument (Bio-Rad). The ribosomal protein S18 (*RPS18*) transcript was employed as the reference gene. Gene expression changes were determined using the ΔΔ-cycle threshold (ΔΔ-Ct) method.

2.11 Statistical Analysis

Data analysis was performed by SPSS 26.0 and GraphPad Prism 10.0 software. Paired t-test for independent means was used for group comparisons. To compare various groups, one-way ANOVA was used, while the Chi-square test was utilized to evaluate the association between LONP1 expression and clinicopathological features. The survival curves were constructed using Kaplan-Meier methodology. Univariate and multivariate ratios of the risk of study factors were analyzed using the Cox proportional hazards regression method. A value of $p \leq 0.05$ was considered statistically significant.

3. Results

3.1 LONP1 expression is elevated in most cancer types

Several lines of evidence have reported an association between the upregulation of LONP1 in several cancers and its involvement in cancer progression and EMT (Zanini *et al.*, 2022). To explore this further, we inspected different publicly available databases to assess LONP1 expression patterns and possible correlations with cancer progression and immune response, particularly in colorectal cancer.

We first inspected the TIMER database. Data analysis showed that LONP1 mRNA tends to be expressed at higher levels in most human cancers (in red) than in normal tissues (in blue), including bladder urothelial carcinoma (BLCA), breast invasive carcinoma (BRCA), cholangiocarcinoma (CHOL), COAD, esophageal carcinoma (ESCA), head and neck squamous cell carcinoma (HNSC), kidney chromophobe (KICH), liver hepatocellular carcinoma (LIHC), lung adenocarcinoma (LUAD), lung squamous cell carcinoma (LUSC), prostate adenocarcinoma (PRAD), rectum adenocarcinoma (READ), stomach adenocarcinoma (STAD), thyroid carcinoma (THCA), and uterine corpus endometrial carcinoma (UCEC) ($p \leq 0.05$). No cancer type showed a consistent decrease in LONP1 expression compared to normal tissues (Fig. 1A). Analysis of the GEPIA2 database gave similar results, as far as COAD was concerned (Fig. 1B). The same significant increase was observed for LONP1 mRNA and protein levels in COAD when compared with normal tissue, as obtained from the UALCAN database (Fig. 1C and 1D).

3.2 A high level of LONP1 expression was closely associated with the malignancy degree of COAD

We previously observed that LONP1 expression linearly increases from normal mucosa to transformed cells in the development of COAD (Gibellini *et al.*, 2018).

For this reason, we inspected the UALCAN database and observed an increment of LONP1 mRNA expression (expressed as transcript per million, TPM) throughout COAD progression (Fig. 2A). The same increment was observed at the protein level (Fig. 2B). We also observed the same increment of LONP1 at the mRNA (Fig. 2C) and protein levels (Fig. 2D) when comparing normal and COAD tissue, based on sex. Both male and female COAD patients showed significantly higher levels of LONP1, while no differences were found between sexes.

Furthermore, LONP1 was found to be differentially expressed based on TP53 mutation status in COAD. As illustrated, the mRNA expression levels of LONP1 were significantly higher in TP53-mutant COAD samples compared with both normal tissues and TP53 wild-type COAD samples (Fig. 2E). These observations suggest a possible association between LONP1 expression and tumor grade or TP53 mutation status, although causality cannot be inferred from these data alone.

Thus, we performed a Kaplan-Meier analysis, using the Kaplan-Meier Plotter online tool, revealing that COAD patients with high LONP1 expression presented no statistically significant difference in overall survival (OS) compared with those with low LONP1 expression (Fig. 3A; p=0.079). Interestingly, subgroup analysis suggested that higher LONP1 expression might be associated with better OS in TP53 wild-type patients (Fig. 3B; p=0.0082) and worse OS in TP53-mutant patients (Fig. 3C; p=0.011). These observations suggest that high levels of LONP1 could further worsen the prognosis in patients with COAD in whom TP53 is mutated.

3.3 LONP1 expression is correlated with proteins regulating mitochondrial functions and dynamics in COAD

We next analyzed the genes co-expressed with LONP1 in COAD patients within the TCGA dataset, using LinkedOmics. Our analysis identified 5,307 genes that significantly correlated with LONP1 expression in colorectal cancer (Fig. 4A; $p < 0.05$ and FDR <0.05). Among them, 1,879 genes showed a positive correlation with LONP1, while 3,428 genes exhibited a negative correlation, as shown in the heat maps (Fig. 4B and 4C). Among the top 50 genes positively associated with LONP1 expression, nine were already known to interact with LONP1 at protein levels, or co-regulated with LONP1 under stress conditions (*ATP5D*, *CLPP*, *MRPL12*, *POLRMT*, *SLC25A10*, *SLC25A39*, *TIMM13*, *TIMM44*, and *TOMM40*). GSEA revealed an association between LONP1 and mitochondrial RNA metabolic process, DNA replication, extracellular structure organization, and neuron projection guidance (Fig. 4D).

Then, we analyzed the relationship at the protein level between LONP1 and other co-expressed proteins in COAD patients within the CPTAC Pancancer dataset, using LinkedOmics. Our analysis identified 1,830 proteins that significantly correlated with LONP1 expression in colorectal cancer (Fig. 4E; $p < 0.05$ and FDR <0.05). Of these, 833 proteins showed a positive correlation with LONP1, while 997 exhibited a negative correlation, as shown in the heat maps (Fig. 4F and 4G). Enrichment analysis revealed an association between LONP1 and mitochondrial transport, mitochondrial membrane organization, muscle system process, and circulatory system process (Fig. 4H).

To confirm these data, we performed a correlation analysis between LONP1 and the genes found to be positively correlated with LONP1, using the TIMER database. We confirmed the positive correlation between LONP1 and mitochondrial proteins, such as ATP5D, CLPP, MRPL12, POLRMT, SLC25A10, SLC25A39, TIMM13, TIMM44, and TOMM40 (Fig. 5). Thus, we investigated the possible correlation between LONP1, and genes related to mitochondrial dynamics, such as *DNM1L*, *FIS1*, *MFN1*, *MFN2*, and *OPA1* (Fig. 6A), and mitophagy, like *AMBRA1*, *BECN1*, *FUNDC1*, *NBR1*, *PARK2*, *PINK1*, and *PTEN* (Fig. 6B). We found that LONP1 expression was negatively correlated with MFN1 and positively correlated with MFN2, suggesting its involvement in mitochondrial dynamics (Fig. 6A). In addition, LONP1 showed a significative positive correlation with AMBRA1 and PINK1 and negative correlation with FUNDC1, PARK2, and PTEN, in agreement with the established role of LONP1 in mitophagy (Fig. 6B).

To validate these observations, we re-analyzed RNA-seq data previously generated in our laboratory from SW620 colorectal cells with silenced LONP1 (Gibellini *et al.*, 2022). As shown in Figure 7, LONP1 silencing in SW620 cells was associated with increased expression of MRPL12, POLRMT, SLC25A10, TIMM13, TIMM44, TOMM40, and TOMM20, confirming the inverse correlation between these gene transcripts and LONP1 levels observed *in silico*. Regarding genes involved in mitochondrial dynamics and morphology, LONP1 silencing resulted in reduced MFN2 transcript levels and increased FUNDC1 and PINK1 transcripts, whereas no significant changes were detected for other genes related to mitochondrial dynamics.

3.4 LONP1 expression levels affect mitochondrial markers, immune cell infiltration, and clinical outcome in CRC

As we noticed that LONP1 is able to modulate PINK1 expression in SW620 cells and is correlated with PINK1 expression (Fig. 6B and 7), we wondered if the expression of LONP1 could affect mitophagy and mitochondrial dynamics *in vivo*, and if this modulation could impact the outcome of the disease.

Thus, we retrospectively selected 50 patients (31 males [62%] and 19 females [38%]; Table 1) with a diagnosis of COAD and monitored the expression of LONP1 and markers of mitophagy and/or mitochondrial dynamics in formalin-fixed, paraffin-embedded (FFPE) specimens via IHC. Due to technical issues with the biopsies, LONP1 expression was analyzed in 48 patients out of 50. The clinical features of enrolled patients and the correlation with LONP1 expression are reported in Table 2. The age at diagnosis ranged from 56 to 89 years (mean age at diagnosis 73 years). In 30 cases, neoplasms originated in the left colon, while in 20 cases, they originated in the right colon. The sizes of the tumor masses ranged from 20 to 70 millimeters (average size approximately 42 mm), and endoscopically/macroscopically, they were excavated/ulcerated in 33 cases (66%) and polypoid-vegetative in 17 (34%). The histotypes consisted of non-acinar subtype (NAS) adenocarcinoma (35 cases; 70%), partially mucinous adenocarcinoma (extracellular mucin <50% of tumor volume, 11 cases; 22%), and mucinous adenocarcinoma (extracellular mucin >50% of tumor volume, 4 cases; 8%). One tumor (2%) was diagnosed at an early stage (Stage 1), 17 (34%) neoplasms were localized to the colonic wall (Stage 2), 23 (46%) neoplasms were locally advanced (N+/Stage 3), and 9 (18%) had metastasized to other organs (M+/Stage 4). Morphological analysis allowed the identification of histological characteristics predictive of an unfavorable prognosis in each tumor. In particular, we selected features with unequivocal pathological significance of aggressiveness, observed in a) tumor grading G3, b) lymph node metastasis related to lymphovascular invasion and tumor budding, c) invasion of the perivisceral serosa, and d) visceral metastasis. All four characteristics were present in five tumors (10%), three were present in four tumors (8%), two were present in 18 tumors (36%), and one was present in 16 tumors (32%). Seven tumors (14%) did not exhibit any of the aforementioned histological unfavorable characteristics.

As expected, IHC for LONP1 was positive in all tumor specimens, in agreement with the ubiquitous expression of the protein. The distribution of the protein was always cytoplasmic, with a weak signal sometimes present in the nucleus. The staining intensity—independently evaluated by two pathologists—ranged from weak (which received a score 1) to strong (which received a score 3). When stratified by gender and tumor features, we observed that LONP1 signal intensity was not associated with gender and tumor grading but was significantly associated with tumor size and position. In particular, we observed that higher signal intensity was present in cancer originating on the left side of the colon, and in smaller cancers (<42 mm).

In the same samples, we next analyzed the expression of markers of mitochondrial mass, mitochondrial dynamics, and mitophagy in the same specimens. The expression of translocase of outer mitochondrial membrane 20 (TOMM20), a typical marker of mitochondrial mass, followed a trend that was inverse with respect to LONP1. This trend was also confirmed in the correlation analysis performed with the TIMER database, showing a significant negative correlation between LONP1 and TOMM20 expression levels (Fig. 8A).

Based on the expression and distribution of Lonp1 and TOMM20 in the 48 samples analyzed, we could distinguish two main patterns. Pattern 1 was characterized by High TOMM20 levels (HTOMM20) and Low LONP1 levels (LLONP1), including weak focal and diffuse expression, and was found in 36 cases. Cases in Pattern 1 comprised 26 advanced-stage tumors (locally advanced with lymph node metastasis or diffusely advanced with lymph node and visceral metastasis) and 10 tumors confined to the colonic visceral wall, all exhibiting at least one feature of malignancy/unfavorable prognosis. Pattern 2 was characterized by Low TOMM20 levels (LTOMM20) and High LONP1 levels (HLONP1), including moderate diffuse and highly diffuse expression, and was observed in the remaining 12 cases. Cases in Pattern 2 included two tumors in a diffusely advanced stage with lymph node and visceral metastasis, four tumors in a locally advanced stage with lymph node metastasis, and six tumors confined to the colonic visceral wall, of which only two exhibited one feature of malignancy/unfavorable prognosis, while four showed no histological characteristics of malignancy. The analysis of available cases suggests a tendency for tumors in Pattern 1 (HTOMM20/LLONP1) to metastasize more frequently and exhibit histological characteristics indicative of malignancy, predisposing to spread and unfavorable prognosis. On the other hand, tumors in Pattern 2 (LTOMM20/HLONP1) appear less likely to display histological characteristics predictive of metastatic spread.

We finally explored the correlation between the immunohistochemical profiles of LONP1 and TOMM20, the clinical-pathological characteristics of the tumors, and the tumor-infiltrating lymphocytes (TIL) in the two group groups (Fig. 8B). Samples displaying Pattern 1 were characterized by multiple histological characteristics of aggressiveness (including metastasis to multiple pericolic lymph nodes), sometimes with distant metastasis (M+), and low or absent TIL (average count 3 T lymphocytes per high-power field [HPF]; hot spot count 5-7 cells per HPF). Conversely, samples displaying Pattern 2 were mostly non-metastatic tumors or with few metastatic lymph nodes (limited to 1-2 lymph nodes), characterized by widespread and intense TIL (average count 25 T lymphocytes per HPF; hot spot count 35-40 T lymphocytes per HPF).

As IHC analysis suggested a possible impact of LONP1 levels on immune cell infiltration, we inspected the TIMER database, looking for a possible association between LONP1 expression and immune markers of different immune cell populations in COAD. LONP1 CNVs exhibited significant correlations with infiltration levels of B cells, CD8+ T cells, neutrophils, and dendritic cells (Fig. 9A). Additionally, we analyzed immune markers of B cells, CD8+ T cells, CD4+ T cells, macrophages, neutrophils, and dendritic cells. After purity-related adjustments, TIMER analysis revealed that LONP1 expression was negatively correlated with the infiltration of B cells, macrophages, and CD8+ T cells—confirming our previous observation—whereas no significant correlation was observed for CD4+ T cells,

neutrophils, and dendritic cells (Fig. 9B). Furthermore, we assessed the impact of LONP1 expression and immune cell infiltration on patient survival outcomes in COAD. As shown in Figure 9C, variations in LONP1 expression within immune cells did not significantly influence the cumulative survival rate of COAD patients over time. Collectively, these findings suggest a potential role for LONP1 in modulating immune cell infiltration in COAD.

To confirm these observations, we also examined the expression of PINK1 and TOMM20 in SW620 cells, either after silencing or overexpressing the full-length form LONP1 (LONP1 Isoform 1, or ISO1). At the mRNA level, we confirmed that LONP1 silencing increased the relative expression of PINK1 in SW620 cells. Conversely, LONP1 overexpression was correlated with reduced expression of PINK1. Regarding TOMM20, silencing of LONP1 did not significantly affect its expression, while its overexpression resulted in slightly reduced relative levels of TOMM20 (Fig. 10).

Because gene–protein correlations were not straightforward in publicly available datasets, particularly as far as PINK1 is concerned, we assessed its expression in the same cell line, either after overexpressing or silencing LONP1. We focused our attention on PINK1, as public data indicated discrepancies between its correlation with LONP1 at the mRNA and protein levels, and previous studies in animal models demonstrated LONP1-mediated degradation of PINK1. Given that PINK1 is expressed at low levels and is barely detectable in these cells in basal conditions, we induced mitophagy by treating cells with CCCP for six hours. As shown in Figure 11A, PINK1 levels increased significantly upon CCCP treatment when LONP1 was silenced, but not when a scrambled siRNA was used. Conversely, LONP1 overexpression in both cell lines prevented PINK1 detection in CCCP-treated cells, indicating that LONP1 promotes PINK1 degradation (Fig. 11B).

Confocal microscopy confirmed that LONP1 silencing followed by CCCP treatment led to PINK1 accumulation in mitochondria in SW620 cells; this effect was minimal in cells treated with control siRNA (Fig. 12A). Overexpression of LONP1 in the same cells led to a reduction in PINK1 signal, which was barely detectable, even though cells were treated with CCCP (Fig. 12B). These experiments were repeated in SW480 cells, yielding similar results (not shown).

4. Discussion

In this study, by combining *in silico* analysis of publicly available datasets and retrospective IHC analysis of specimens from patients with COAD, we showed that LONP1 is upregulated in tumor tissues compared with normal counterparts. Moreover, we demonstrated that its levels are correlated with tumor progression, mitochondrial dynamics, and immune infiltration. Our findings suggest that LONP1 may serve as a potential biomarker for COAD prognosis and a key regulator of mitochondrial homeostasis in cancer cells.

We first observed that LONP1 expression is significantly higher in COAD than in normal tissues, as confirmed by database analyses and IHC. This observation is in agreement with previous reports on the role of LONP1 in cancer progression and further confirms its involvement in tumor cell adaptation to metabolic and oxidative stress (Gibellini *et al.*, 2018).

Furthermore, LONP1 levels were positively associated with TP53 mutations, particularly in tumors with poor prognosis. In agreement with this observation, our previous study highlighted that LONP1 is preferentially upregulated in CRC samples with mutated P53 (Gibellini *et al.*, 2018). The interaction(s) between LONp1 and p53 are quite complex and not completely elucidated. On one side, LONP1 interacts with p53 in the mitochondrial matrix, mitigating p53-induced apoptosis under oxidative stress, and impairs the transcription-dependent apoptotic function of p53 by reducing the mRNA expression of its target genes. On the other side, mitochondrial LONP1 enhances the stability and abundance of p53 (Sung *et al.*, 2018). However, no information is currently available regarding the effect of p53 levels on *LONP1* transcription. We can speculate that the higher levels of LONP1 transcripts in the presence of TP53 mutations could be due to a lower capability of p53 mutant cells to cope with oxidative or endoplasmic reticular stress, which can induce *LONP1* transcription (Gibellini *et al.*, 2020). Further studies are needed to clarify this point.

Concerning mitochondrial functionality and dynamics, our observations are in line with some known roles of LONP1. LONP1 transcriptional levels are increased when mitogenesis is promoted, and this notion is confirmed by the positive correlation between LONP1 and POLMRT, the gene whose product is crucial for mtDNA transcription and initiation of replication, or ATP5D, a subunit of mitochondrial ATP synthase. Furthermore, LONP1 expression is positively correlated with that of CLPP, another mitochondrial matrix protease often co-regulated with LONP1 (Zhang *et al.*, 2023).

The observed correlation between LONP1 and mitophagy-related proteins, such as PINK1 and AMBRA1, supports its role in mitochondrial quality control mechanisms and as a regulator of mitophagy. Studies have established the interrelation between LONP1 and PINK1, indicating that the loss of LONP1 function can lead to the accumulation of PINK1, suggesting a feedback mechanism where LONP1 potentially regulates PINK1-mediated pathways (Thomas *et al.*, 2014; Zurita Rendon and Shoubridge, 2018). The absence of LONP1 results in enhanced PINK1-Parkin activity (Liu et al.), which is linked to increased mitophagy and may counteract mitochondrial dysfunctions associated with aging and neurodegenerative conditions (Thomas *et al.*, 2014). We observed a positive correlation between LONP1 and PINK1 at the transcriptional level, likely related to higher mitochondrial mass or number, rather than increased mitophagy, whose regulation occurs at the protein level through LONP1-mediated degradation of LONP1. We could not detect PINK1 expression at the protein level in our IHC analysis, likely because the steady levels of PINK1 are generally very low. Interestingly, the negative correlation between LONP1 and TOMM20 expression suggests that tumors with high LONP1 levels may undergo increased mitochondrial turnover, potentially promoting cancer cell survival.

Additionally, the link between LONP1 and immune infiltration markers revealed an inverse association with CD8+ T cells, suggesting a potential role in immune evasion mechanisms. The two immunohistochemical expression patterns we identified—high LONP1/low TOMM20 in aggressive tumors and low LONP1/high TOMM20 in less invasive cases—further support the impact of LONP1 on COAD progression and patient prognosis.

Despite these insights, our study has some limitations. The findings presented here are primarily based on analyses of publicly available datasets, which, although comprehensive, are inherently correlative and subject to biases in sample collection and processing. The observed associations between LONP1 expression, cancer progression, and mitochondrial-related genes cannot establish causality and may be influenced by confounding factors such as tumor heterogeneity, treatment history, and patient demographics. Furthermore, protein-level data from CPTAC and other resources, while informative, may not fully capture post-translational modifications or functional activity of LONP1. Survival analyses should be interpreted with caution, as they rely on retrospective data and may not account for all clinical variables influencing patient outcomes. The sample size of 50 COAD cases, while informative, remains relatively small, and validation in larger, independent cohorts is needed. Additionally, further functional studies are necessary to elucidate the precise molecular mechanisms through which LONP1 influences mitophagy, immune modulation, and cancer metabolism.

While our study integrates *in silico* analyses with *in vitro* validation in CRC cell lines, we acknowledge the importance of further functional studies using stable knockout or knockdown models. However, to fully elucidate the mechanistic role of LONP1 in tumor progression and immune modulation, future studies will focus on the generation of stable KO/KD models in CRC cell lines. These models will allow for long-term functional assays, including metabolic profiling, mitochondrial dynamics, and immune cell co-culture systems to assess the impact of LONP1 on tumor-immune interactions. Given the embryonic lethality of complete LONP1 knockout *in vivo*, as previously reported (De Gaetano *et al.*, 2020). Conditional or tissue-specific KO mouse models may provide a viable strategy to investigate the role of LONP1 in colorectal tumorigenesis and immune evasion in a physiological context. These approaches will be instrumental in validating LONP1 as a potential therapeutic target and in exploring its utility in combination with immunotherapeutic strategies.

5. Conclusions

The findings of our study indicate a notable association between elevated levels of LONP1 and an unfavorable prognosis in COAD. Additionally, LONP1 is strongly correlated with proteins involved in mitophagy and mitochondrial dynamics, suggesting its potential role in modulating mitochondrial function and contributing to COAD progression. The analysis reveals that LONP1 is significantly linked to various signaling pathways, including those related to mitochondrial homeostasis and cellular stress responses. In aggregate, our findings highlight the potential of LONP1 as a promising prognostic biomarker for COAD. Furthermore, its involvement in mitochondrial dynamics confirms LONP1 as a promising target for therapeutic interventions aimed at regulating mitochondrial function in the context of colon adenocarcinoma.

Author Contributions: Conceptualization, M.P. and L.R.B.; methodology, G.Z. and S.C.; formal analysis, G.Z., V.S., and G.M.; investigation, G.Z., V.S., G.S, G.M., I.M., S.C., and L.R.B.; data curation, G.Z., V.S., G.S., G.M, I.M., and M.N.; writing—original draft preparation, G.Z., L.R.B., and M.P.; writing—review and editing, G.Z., M.N., S.C., L.R.B., and M.P.; supervision, L.R.B and M.P.; project administration, M.P.; funding acquisition, M.P. All authors have read and agreed to the published version of the manuscript.

Funding: The research leading to these results has received funding from AIRC under IG 2017 ID. 19786 and IG 2024 ID. 30707 projects – P.I. Pinti Marcello

The authors declare no conflict of interest.

Legends to figures

Figure 1. LONP1 is expressed at high levels in cancer. A. Expression levels of LONP1 mRNA in different types of cancers (red), in comparison with normal tissue counterparts (blue), as reported in the TIMER database. COAD is highlighted by a red box. Data are shown as log2 transcript per million (TPM). **= p<0.001; ***= p<0.0001. **B.** Expression levels of LONP1 mRNA in tumor samples (T, depicted in red) and normal tissue (N, depicted in gray) according to the GEPIA2 database. COAD is highlighted by a red box and reported in a single boxplot on the right. Data are shown as log2 TPM. **= p<0.001. **C.** Expression of LONP1 mRNA in COAD primary tumor (depicted in red) in comparison to normal tissue counterpart (depicted in blue), as reported in the TCGA database. Data are shown as TPM. **D.** Expression of LONP1 protein in COAD primary tumor (depicted in red) in comparison to its normal tissue counterpart (depicted in blue), as reported in the CPTAC database. Z-values represent standard deviations from the median across samples for the given cancer type. Log2 Spectral count ratio values from CPTAC were first normalized within each sample profile, then normalized across samples.

Figure 2. LONP1 is expressed at high levels during COAD progression. A. Expression levels of LONP1 mRNA during COAD progression (Stage 1 in orange, Stage 2 in brown, Stage 3 in green, Stage 4 in red), in comparison with normal tissue counterparts (depicted in blue), as reported in the UALCAN database. Data are shown as TPM. **B.** Protein levels of LONP1 during COAD progression (Stage 1 in orange, Stage 2 in brown, Stage 3 in green, Stage 4 in red), in comparison with normal tissue counterparts (depicted in blue), as reported in the UALCAN database. Data are shown as Z-values. **C.** LONP1 mRNA expression levels in COAD based on patients' gender (male depicted in red and female depicted in orange) in comparison with normal tissue counterparts (depicted in blue), as reported in the UALCAN database. Data are shown as TPM. **D.** LONP1 protein levels in COAD based on patients' gender (male depicted in red and female depicted in orange) in comparison with normal tissue counterparts (depicted in blue), as reported in the UALCAN database. Data are shown

as Z-values. **E.** mRNA expression levels of LONP1 in TP53-mutant COAD in normal tissues and non-mutant COAD. Data are shown as TPM.

Figure 3. High levels of LONP1 were associated with a poor prognosis in COAD patients. A. Kaplan-Meier survival curves showing the association between LONP1 levels and survival probability in COAD patients. **B.** Kaplan-Meier survival curves showing the association between LONP1 levels and survival probability in COAD patients with wild-type P53. **C.** Kaplan-Meier survival curves showing the association between LONP1 levels and survival probability in COAD patients with mutated P53.

Figure 4. LinkedOmics database and enrichment analysis were used to examine LONP1 co-expression genes in COAD. A. Vulcano plot showing highly associated *LONP1* genes in a COAD cohort. **B.** Heatmap with the top 50 genes positively associated with LONP1 expression. **C.** Heatmap with the top 50 genes negatively associated with LONP1 expression. **D.** Representative GO enrichment plots for positively and negatively enriched pathways with LONP1 expression. **E.** Vulcano plot showing highly associated LONP1 proteins in a COAD cohort. **F.** Heatmap with the top 50 proteins positively associated with LONP1. **G.** Heatmap with the top 50 proteins negatively associated with LONP1. **H.** Representative GO enrichment plots for positively and negatively enriched pathways with LONP1.

Figure 5. Correlation between LONP1 and mitochondrial factors. Analysis of correlation between LONP1 and mitochondrial factors already known to interact or co-regulate with LONP1, present in the most significant 50 genes positively correlated to LONP1 from the LinkedOmics database (*ATP5D*, *CLPP*, *MRPL12*, *POLRMT*, *SLC25A10*, *SLC25A39*, *TIMM13*, *TIMM44*, and *TOMM40*).

Figure 6. Correlation between LONP1 and mitochondrial dynamics and mitophagy factors. A. Analysis of correlation between LONP1 and mitochondrial dynamics factors (DNM1L, FIS1, MFN1, MFN2, OPA1). **B.** Analysis of correlation between LONP1 and mitophagy factors (AMBRA1, BECN1, FUNDC1, NBR1, PARK2, PINK1, and PTEN).

Figure 7. LONP1 silencing modulates the expression of mitochondrial genes in colorectal cancer cells. A. Relative mRNA expression levels of mitochondrial genes in SW620 cells after LONP1 silencing, as determined by RNAseq analysis. Genes positively correlated with LONP1 in *in silico* analyses (e.g., *MRPL12*, *POLRMT*, *SLC25A10*, *TIMM13*, *TIMM44*, *TOMM40*, and *TOMM20*) were upregulated upon LONP1 silencing, while negatively correlated genes (e.g., *MFN2*, *FUNDC1*, and *PINK1*) showed inverse expression patterns. Data are shown as **= $p<0.001$; ***= $p<0.0001$.

Figure 8. Correlation between the immunohistochemical profiles of Lonp1 and TOMM20 and lymphocyte infiltration in the tumor mass. A. Analysis of the correlation between LONP1 and TOMM20. **B.** Representative IHC images of COAD with different levels of TOMM20, LONP1, and TIL.

Figure 9. LONP1-related immune infiltration in COAD. A. LONP1 CNVs effect on the infiltration levels of B cells, CD8+ T cells, neutrophils, and dendritic cells in COAD (*p<0.05, **p<0.01). **B.** Correlation between LONP1 expression and immune markers of different immune cells in COAD. **C.** Correlation of cumulative survival rate and immune infiltration, including B cells, CD8+T cells, CD4+T cells, macrophages, neutrophils, and DCs in COAD.

Figure 10. LONP1 silencing or overexpression affects PINK1 and TOMM20 expression in SW620 cells. A. Quantitative real-time PCR analysis of LONP1, PINK1, and TOMM20 mRNA levels in SW620 cells after LONP1 silencing (siRNA) or overexpression (ISO1). LONP1 silencing increased PINK1 expression and had minimal effects on TOMM20, while overexpression reduced PINK1 and slightly decreased TOMM20 levels. Data are shown as relative expression normalized to RPS18, and are presented as mean ± SD of three independent experiments, **= p<0.001; ***= p<0.0001.

Figure 11. LONP1 regulates PINK1 protein levels in colorectal cancer cells. A. Western blot analysis and histograms showing relative protein levels of PINK1 and LONP1 in SW620 cells treated with CCCP to induce mitophagy, following LONP1 silencing. LONP1 silencing led to increased PINK1 accumulation, while overexpression suppressed PINK1 levels. Data are reported as mean ± SD of three independent experiments, *= p<0.05. **B.** Western blot analysis and histograms showing relative protein levels of PINK1 and LONP1 in SW620 stably overexpressing LONP1, with or without treatment with CCCP to induce mitophagy. Data are reported as mean ± SD of three independent experiments, *= p<0.05.

Figure 12. LONP1 regulates PINK1 localization in colorectal cancer cells. A. Confocal microscopy images showing PINK1 localization in SW620 cells after LONP1 silencing or overexpression, after treatment with CCCP. PINK1 (green), mitochondria (hMit, red), and nuclei (DAPI, blue). Merged images show PINK1 accumulation at mitochondria upon LONP1 silencing. Length bar = 10 µm. **B.** Confocal microscopy images showing PINK1 localization in SW620 cells after LONP1 overexpression, after treatment with CCCP. PINK1 (green), mitochondria (hMit, red), and nuclei (DAPI, blue). Merged images show PINK1 accumulation at mitochondria upon LONP1 silencing. LONP1 silencing enhances PINK1 mitochondrial localization, while overexpression reduces it. Length bar = 10 µm.

Table 1. Clinical features of the 50 enrolled patients.

Table 2. Expression of LONP1 evaluated by IHC in 48/50 cases of colorectal cancer, stratified according to gender, tumor size, location, and grading. Significant differences are highlighted in bold.

Feature	**N (%)**
Sex	31 males/19 females
Age at diagnosis (mean±SD)	73 ± 17 years
Average macroscopic size of neoplasms	42 mm (range 20-70 mm*):*
Tumor histotypes	
Mucinous/colloid/ring with stone COAD	4
Martially mucinous COAD	11
NAS COAD	35
Stage at diagnosis	
Early stage (Stage 1)	1
Localized to the colonic wall (Stage 1 and 2)	17
Locally advanced (Stage 3)	23
Metastatic to visceral organs (Stage 4)	9
Tumor growth pattern	
Excavated/ulcerated	33
Polypoid-vegetative	17
Histological features predictive of unfavorable prognosis	
No features	7
Presence of one feature	16
Presence of two features	18
Presence of three features	4
Presence of four features	5

Table 1. Histological features of the 50 COAD cases studied**.**

Feature value	N (%)	LONP1 Expression				*p*-value
		0	1	2	3	
Patients	48	0	19	22	7	
Gender						
M	31 (62%)	0	14	14	3	0.331
F	17 (38%)	0	5	8	4	
Tumor size						
<4.2 cm	28	0	9	12	7	**<0.05**
>4.2 cm	20	0	11	9	0	
Tumor location						
Right	19	0	12	6	1	**<0.05**
Left	29	0	7	16	6	
Tumor grading						
G1	*1*	0	0	1	0	0.583
G2	29	0	10	15	4	
G3	18	0	9	6	3	

Table 2. Expression of LONP1 as evaluated by IHC and correlation with clinical parameters in the selected COAD cases. Quantification of LONP1 was possible only in 48 out of 50 cases selected.

Bibliography

Bernstein S.H., Venkatesh S., Li M., Lee J., Lu B., Hilchey S.P., Morse K.M., Metcalfe H.M., Skalska J., Andreeff M., Brookes P.S. and Suzuki C.K. (2012). The mitochondrial ATP-dependent lon protease: A novel target in lymphoma death mediated by the synthetic triterpenoid cddo and its derivatives. Blood 119, 3321-3329.

Cheng C.W., Kuo C.Y., Fan C.C., Fang W.C., Jiang S.S., Lo Y.K., Wang T.Y., Kao M.C. and Lee A.Y. (2013). Overexpression of lon contributes to survival and aggressive phenotype of cancer cells through mitochondrial complex I-mediated generation of reactive oxygen species. Cell. Death Dis. 4, e681.

De Gaetano A., Gibellini L., Bianchini E., Borella R., De Biasi S., Nasi M., Boraldi F., Cossarizza A. and Pinti M. (2020). Impaired mitochondrial morphology and functionality in *Lonp1*$^{wt/-}$ mice. J. Clin. Med. 9, 1783.

Di K., Lomeli N., Wood S.D., Vanderwal C.D. and Bota D.A. (2016). Mitochondrial lon is over-expressed in high-grade gliomas, and mediates hypoxic adaptation: Potential role of lon as a therapeutic target in glioma. Oncotarget 7, 77457-77467.

Edge S.B., American Joint Committee on Cancer. and American Cancer Society. (2010). Ajcc cancer staging handbook : From the ajcc cancer staging manual, 7th ed. Springer. New York.

Gibellini L., Losi L., De Biasi S., Nasi M., Lo Tartaro D., Pecorini S., Patergnani S., Pinton P., De Gaetano A., Carnevale G., Pisciotta A., Mariani F., Roncucci L., Iannone A., Cossarizza A. and Pinti M. (2018). Lonp1 differently modulates mitochondrial function and bioenergetics of primary versus metastatic colon cancer cells. Front. Oncol. 8, 254.

Gibellini L., De Gaetano A., Mandrioli M., Van Tongeren E., Bortolotti C.A., Cossarizza A. and Pinti M. (2020). The biology of Lonp1: More than a mitochondrial protease. Int. Rev. Cell Mol. Biol. 354, 1-61.

Gibellini L., Borella R., De Gaetano A., Zanini G., Tartaro D.L., Carnevale G., Beretti F., Losi L., De Biasi S., Nasi M., Forcato M., Cossarizza A. and Pinti M. (2022). Evidence for mitochondrial Lonp1 expression in the nucleus. Sci. Rep. 12, 10877.

Győrffy B. (2024). Integrated analysis of public datasets for the discovery and validation of survival-associated genes in solid tumors. Innovation (Camb) 5, 100625.

Lazarou M., Sliter D.A., Kane L.A., Sarraf S.A., Wang C., Burman J.L., Sideris D.P., Fogel A.I. and Youle R.J. (2015). The ubiquitin kinase PINK1 recruits autophagy receptors to induce mitophagy. Nature 524, 309-314.

Li T., Fan J., Wang B., Traugh N., Chen Q., Liu J.S., Li B. and Liu X.S. (2017). TIMER: A web server for comprehensive analysis of tumor-infiltrating immune cells. Cancer Res. 77, e108-e110.

Li J., Agarwal E., Bertolini I., Seo J.H., Caino M.C., Ghosh J.C., Kossenkov A.V., Liu Q., Tang H.Y., Goldman A.R., Languino L.R., Speicher D.W. and Altieri D.C. (2020). The mitophagy effector FUNDC1 controls mitochondrial reprogramming and cellular plasticity in cancer cells. Sci. Signal 13, eaaz8240.

Liu L., Feng D., Chen G., Chen M., Zheng Q., Song P., Ma Q., Zhu C., Wang R., Qi W., Huang L., Xue P., Li B., Wang X., Jin H., Wang J., Yang F., Liu P., Zhu Y., Sui S. and Chen Q. (2012). Mitochondrial outer-membrane protein FUNDC1 mediates hypoxia-induced mitophagy in mammalian cells. Nat. Cell Biol. 14, 177-185.

Liu Y., Lan L., Huang K., Wang R., Xu C., Shi Y., Wu X., Wu Z., Zhang J., Chen L., Wang L., Yu X., Zhu H. and Lu B. (2014). Inhibition of lon blocks cell proliferation, enhances chemosensitivity by promoting apoptosis and decreases cellular bioenergetics of bladder cancer: Potential roles of lon as a prognostic marker and therapeutic target in baldder cancer. Oncotarget 5, 11209-11224.

Lokuhetty D., White V.A., Watanabe R., Cree I.A., World Health Organization. and International Agency for Research on Cancer. (Digestive system tumours, Fifth edition. ed.

Nie X., Li M., Lu B., Zhang Y., Lan L., Chen L. and Lu J. (2013). Down-regulating overexpressed human lon in cervical cancer suppresses cell proliferation and bioenergetics. PLoS One 8, e81084.

Pinti M., Gibellini L., De Biasi S., Nasi M., Roat E., O'Connor J.E. and Cossarizza A. (2011). Functional characterization of the promoter of the human lon protease gene. Mitochondrion 11, 200-206.

Quiros P.M., Espanol Y., Acin-Perez R., Rodriguez F., Barcena C., Watanabe K., Calvo E., Loureiro M., Fernandez-Garcia M.S., Fueyo A., Vazquez J., Enriquez J.A. and Lopez-Otin C. (2014). ATP-dependent lon protease controls tumor bioenergetics by reprogramming mitochondrial activity. Cell Rep. 8, 542-556.

Sung Y.J., Kao T.Y., Kuo C.L., Fan C.C., Cheng A.N., Fang W.C., Chou H.Y., Lo Y.K., Chen C.H., Jiang S.S., Chang I.S., Hsu C.H., Lee J.C. and Lee A.Y. (2018). Mitochondrial lon sequesters and stabilizes p53 in the matrix to restrain apoptosis under oxidative stress via its chaperone activity. Cell Death Dis. 9, 697.

Tanaka A., Cleland M.M., Xu S., Narendra D.P., Suen D.F., Karbowski M. and Youle R.J. (2010). Proteasome and p97 mediate mitophagy and degradation of mitofusins induced by parkin. J. Cell Biol. 191, 1367-1380.

Tang Z., Kang B., Li C., Chen T. and Zhang Z. (2019). GEPIA2: An enhanced web server for large-scale expression profiling and interactive analysis. Nucleic Acids Res. 47, W556-W560.

Thomas R.E., Andrews L.A., Burman J.L., Lin W.Y. and Pallanck L.J. (2014). PINK1-Parkin pathway activity is regulated by degradation of PINK1 in the mitochondrial matrix. PLoS Genet. 10, e1004279.

Yoo S.M. and Jung Y.K. (2018). A molecular approach to mitophagy and mitochondrial dynamics. Mol. Cells 41, 18-26.

Zanini G., Selleri V., De Gaetano A., Gibellini L., Malerba M., Mattioli A.V., Nasi M., Apostolova N. and Pinti M. (2022). Differential expression of lonp1 isoforms in cancer cells. Cells 11, 3940.

Zhang J., Qiao W. and Luo Y. (2023). Mitochondrial quality control proteases and their modulation for cancer therapy. Med. Res. Rev. 43, 399-436.

Zurita Rendon O. and Shoubridge E.A. (2018). LONP1 is required for maturation of a subset of mitochondrial proteins, and its loss elicits an integrated stress response. Mol. Cell Biol. 38, e00412-17.

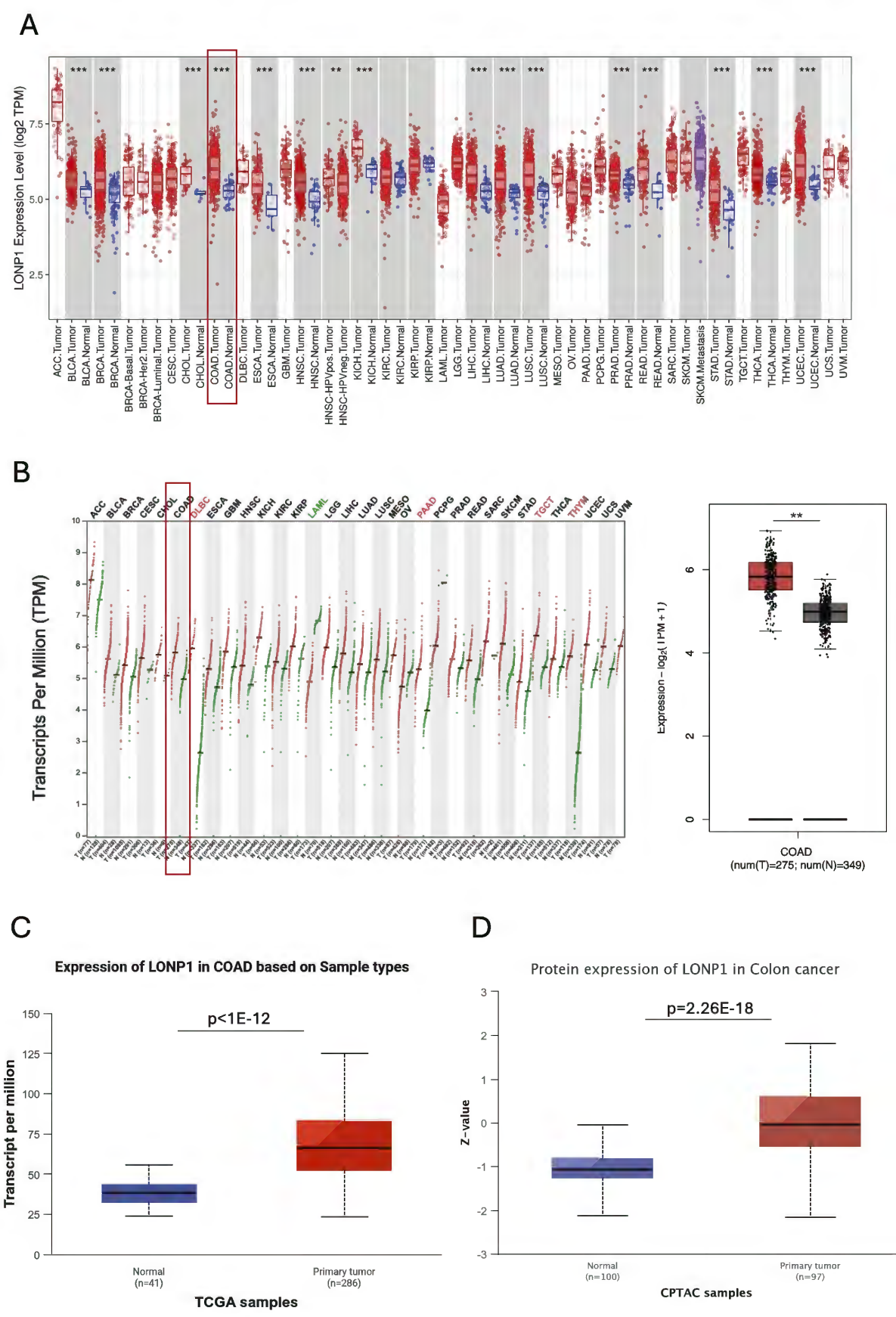
A
LONP1 Expression Level (log2 TPM)
7.5
5.0
2.5
ACC.Tumor
BLCA.Tumor
BLCA.Normal
BRCA.Tumor
BRCA.Normal
BRCA-Basal.Tumor
BRCA-Her2.Tumor
BRCA-Luminal.Tumor
CESC.Tumor
CHOL.Tumor
CHOL.Normal
COAD.Tumor
COAD.Normal
DLBC.Tumor
ESCA.Tumor
ESCA.Normal
GBM.Tumor
HNSC.Tumor
HNSC.Normal
HNSC-HPVpos.Tumor
HNSC-HPVneg.Tumor
KICH.Tumor
KICH.Normal
KIRC.Tumor
KIRC.Normal
KIRP.Tumor
KIRP.Normal
LAML.Tumor
LGG.Tumor
LIHC.Tumor
LIHC.Normal
LUAD.Tumor
LUAD.Normal
LUSC.Tumor
LUSC.Normal
MESO.Tumor
OV.Tumor
PAAD.Tumor
PCPG.Tumor
PRAD.Tumor
PRAD.Normal
READ.Tumor
READ.Normal
SARC.Tumor
SKCM.Tumor
SKCM.Metastasis
STAD.Tumor
STAD.Normal
TGCT.Tumor
THCA.Tumor
THCA.Normal
THYM.Tumor
UCEC.Tumor
UCEC.Normal
UCS.Tumor
UVM.Tumor
B
Transcripts Per Million (TPM)
Expression – log2(TPM + 1)
COAD
(num(T)=275; num(N)=349)
C
Expression of LONP1 in COAD based on Sample types
p<1E-12
Transcript per million
Normal
(n=41)
Primary tumor
(n=286)
TCGA samples
D
Protein expression of LONP1 in Colon cancer
p=2.26E-18
Z-value
Normal
(n=100)
Primary tumor
(n=97)
CPTAC samples

A

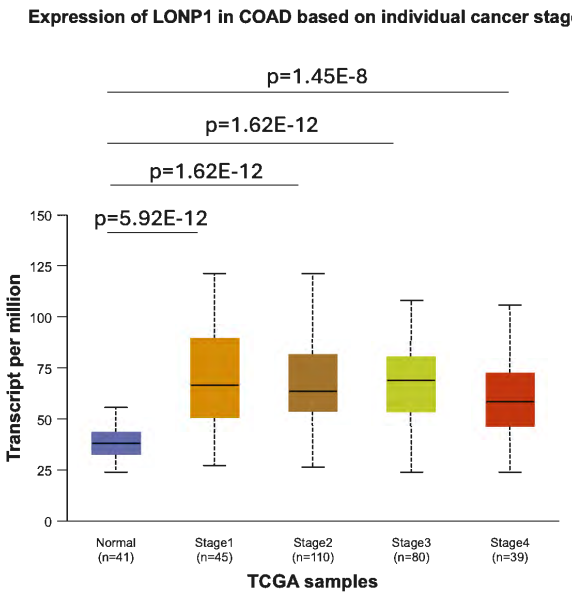

B

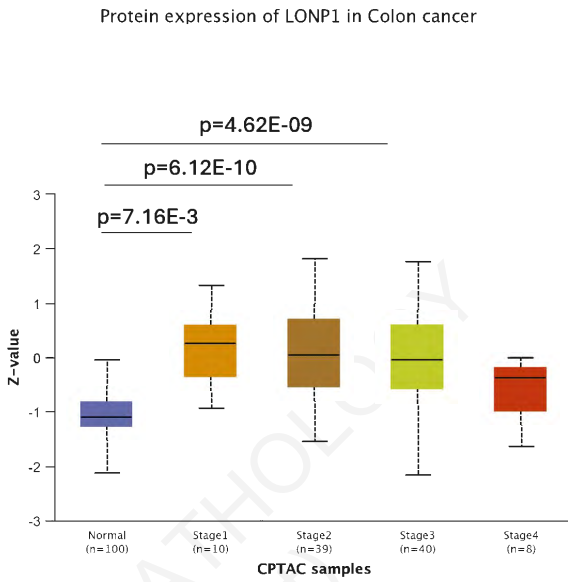

C

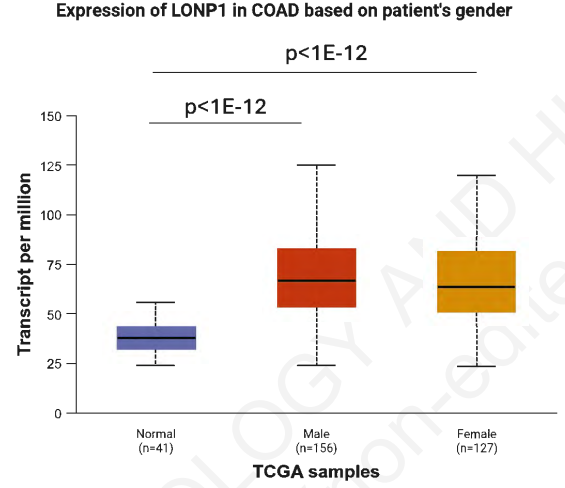

D

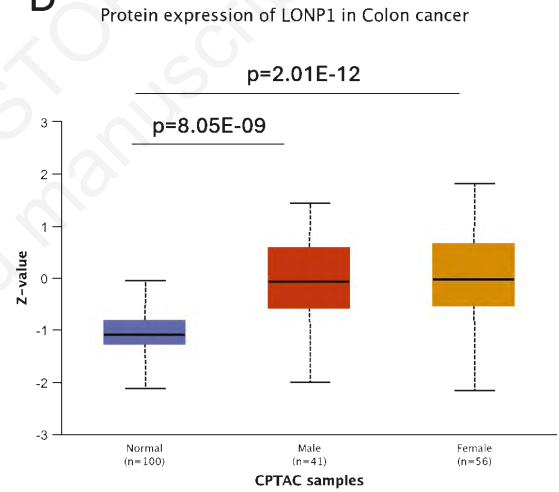

E

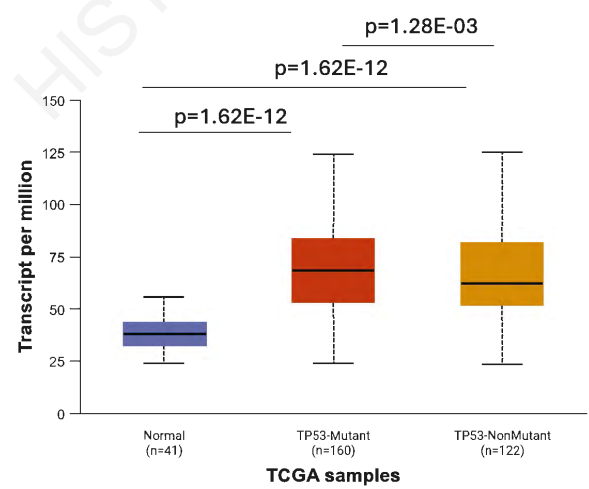

A

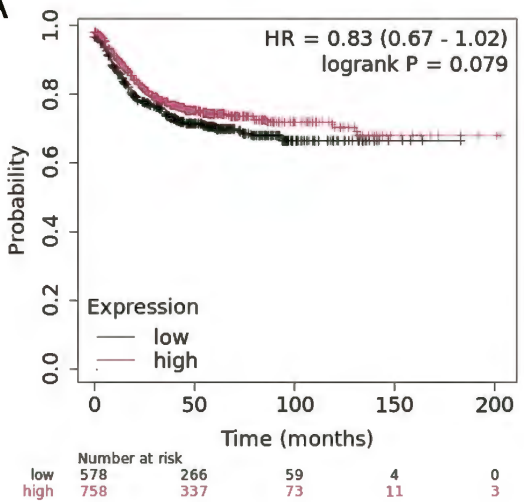
HR = 0.83 (0.67 - 1.02)
logrank P = 0.079
Probability
Expression
low
high
Time (months)
Number at risk
low 578 266 59 4 0
high 758 337 73 11 3

B

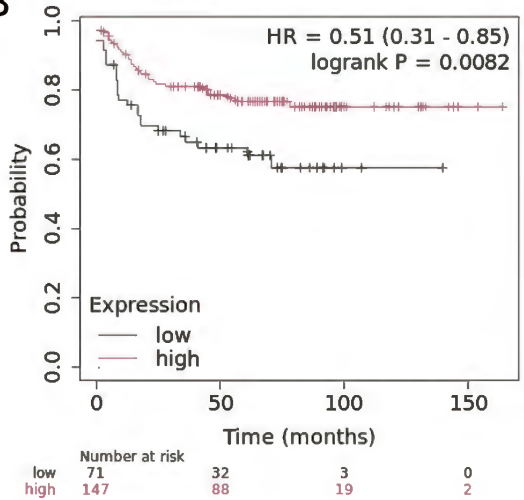
LONP1 (209017_s_at)
HR = 0.51 (0.31 - 0.85)
logrank P = 0.0082
Probability
Expression
low
high
Time (months)
Number at risk
low 71 32 3 0
high 147 88 19 2

C

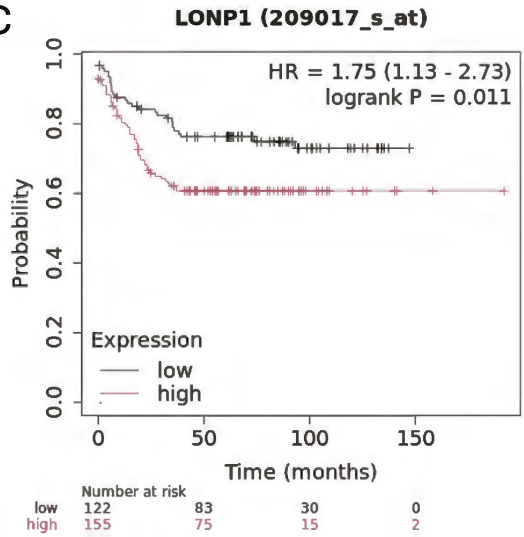
LONP1 (209017_s_at)
HR = 1.75 (1.13 - 2.73)
logrank P = 0.011
Probability
Expression
low
high
Time (months)
Number at risk
low 122 83 30 0
high 155 75 15 2

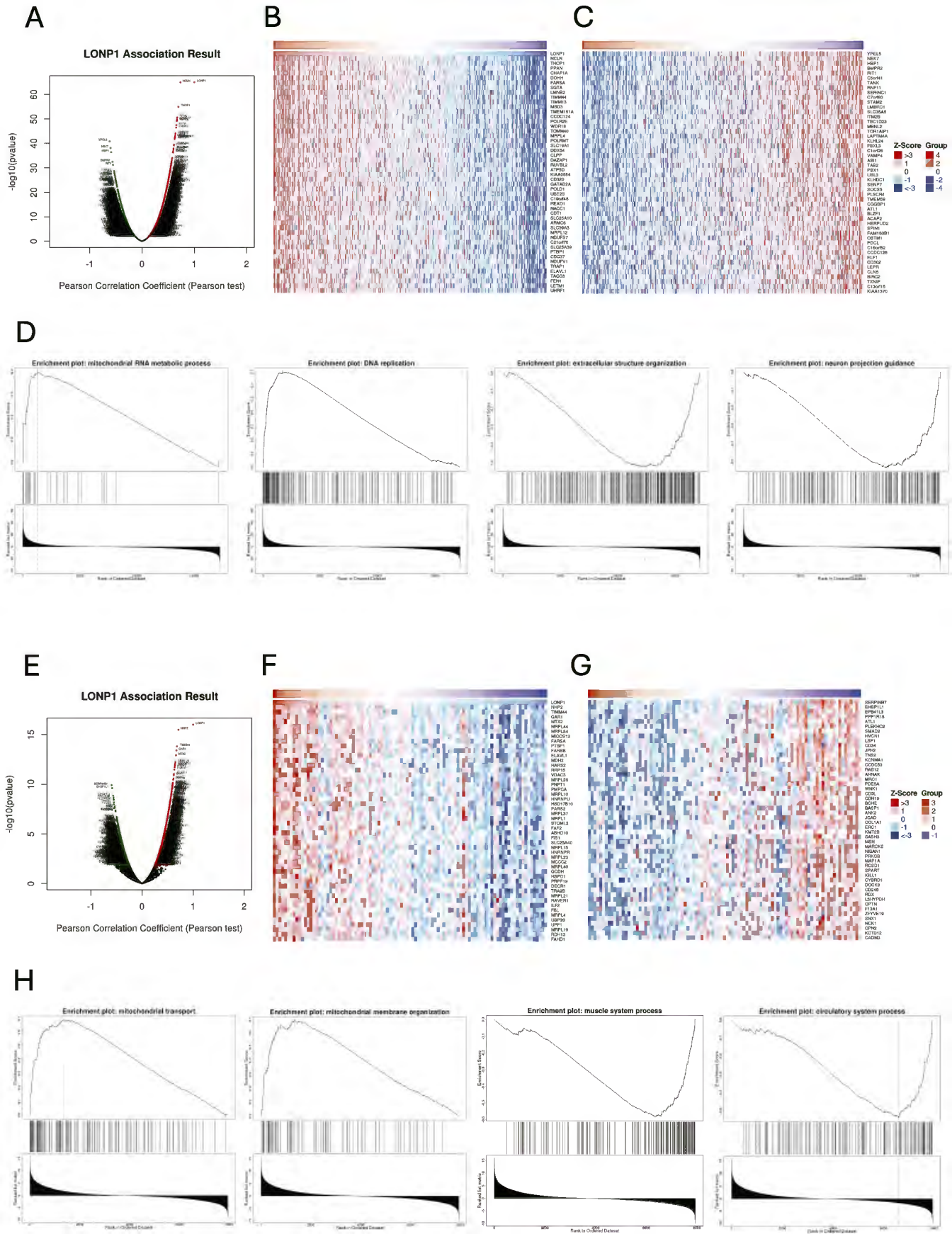
A
LONP1 Association Result
-log10(pvalue)
Pearson Correlation Coefficient (Pearson test)
B
C
Z-Score
Group
D
Enrichment plot: mitochondrial RNA metabolic process
Enrichment plot: DNA replication
Enrichment plot: extracellular structure organization
Enrichment plot: neuron projection guidance
E
LONP1 Association Result
-log10(pvalue)
Pearson Correlation Coefficient (Pearson test)
F
G
Z-Score
Group
H
Enrichment plot: mitochondrial transport
Enrichment plot: mitochondrial membrane organization
Enrichment plot: muscle system process
Enrichment plot: circulatory system process

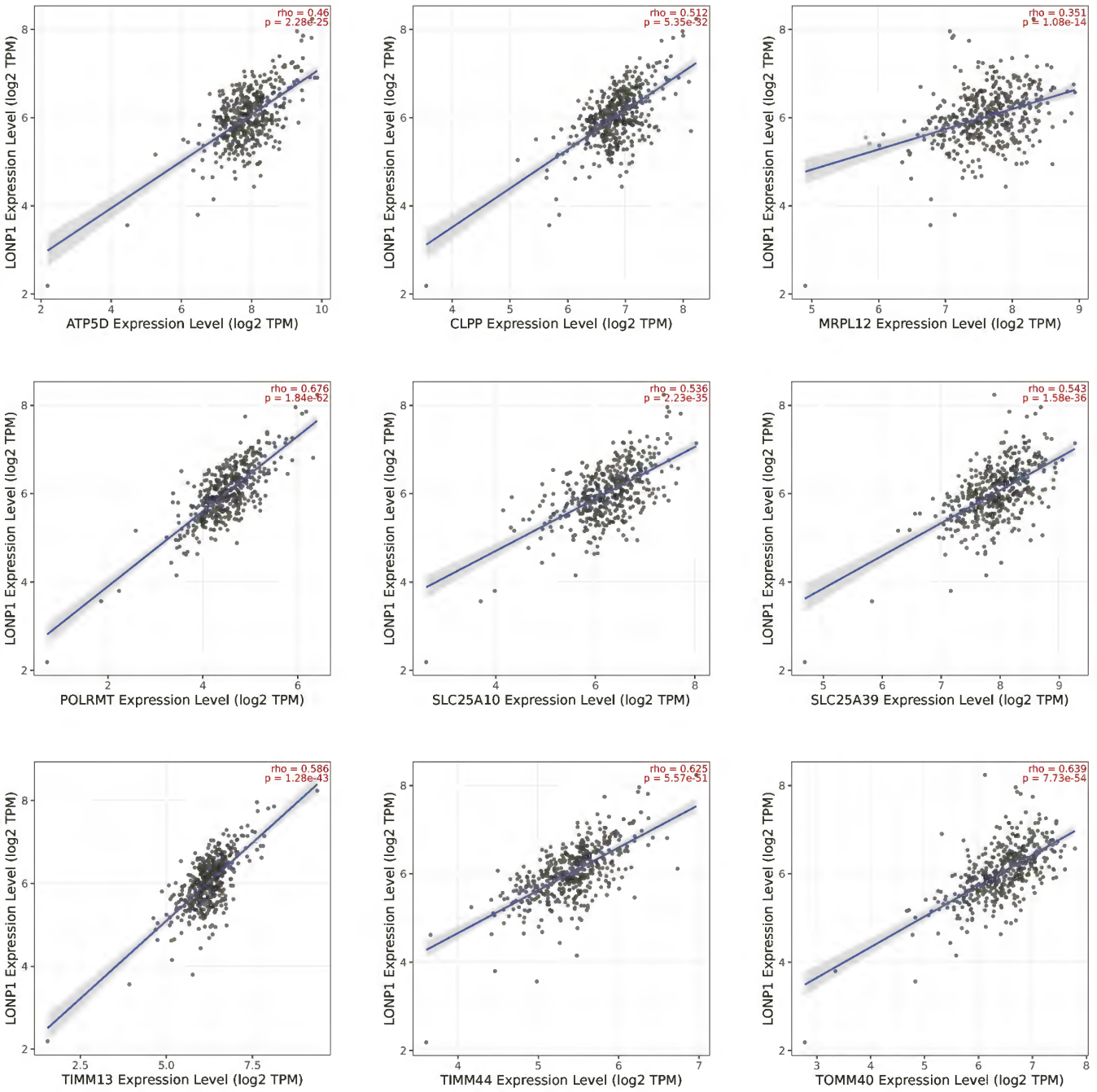
rho = 0.46
p = 2.28e-25
LONP1 Expression Level (log2 TPM)
ATP5D Expression Level (log2 TPM)
rho = 0.512
p = 5.35e-32
LONP1 Expression Level (log2 TPM)
CLPP Expression Level (log2 TPM)
rho = 0.351
p = 1.08e-14
LONP1 Expression Level (log2 TPM)
MRPL12 Expression Level (log2 TPM)
rho = 0.676
p = 1.84e-62
LONP1 Expression Level (log2 TPM)
POLRMT Expression Level (log2 TPM)
rho = 0.536
p = 2.23e-35
LONP1 Expression Level (log2 TPM)
SLC25A10 Expression Level (log2 TPM)
rho = 0.543
p = 1.58e-36
LONP1 Expression Level (log2 TPM)
SLC25A39 Expression Level (log2 TPM)
rho = 0.586
p = 1.28e-43
LONP1 Expression Level (log2 TPM)
TIMM13 Expression Level (log2 TPM)
rho = 0.625
p = 5.57e-51
LONP1 Expression Level (log2 TPM)
TIMM44 Expression Level (log2 TPM)
rho = 0.639
p = 7.73e-54
LONP1 Expression Level (log2 TPM)
TOMM40 Expression Level (log2 TPM)

A

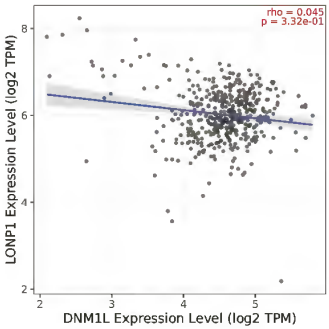
rho = 0.045
p = 3.32e-01
LONP1 Expression Level (log2 TPM)
DNM1L Expression Level (log2 TPM)

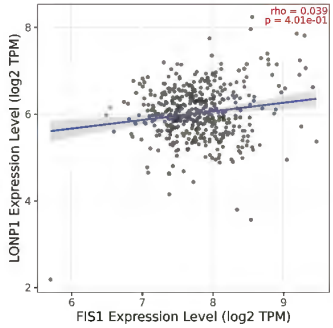
rho = 0.039
p = 4.01e-01
LONP1 Expression Level (log2 TPM)
FIS1 Expression Level (log2 TPM)

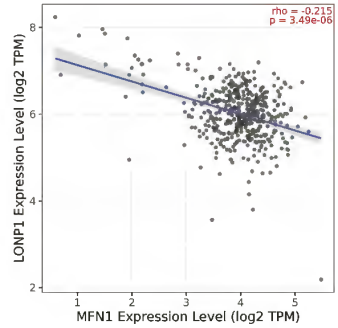
rho = -0.215
p = 3.49e-06
LONP1 Expression Level (log2 TPM)
MFN1 Expression Level (log2 TPM)

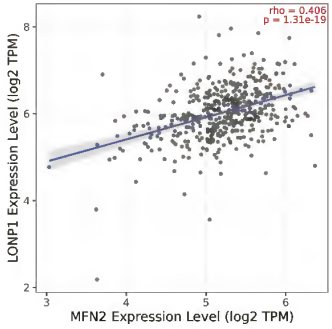
rho = 0.406
p = 1.31e-19
LONP1 Expression Level (log2 TPM)
MFN2 Expression Level (log2 TPM)

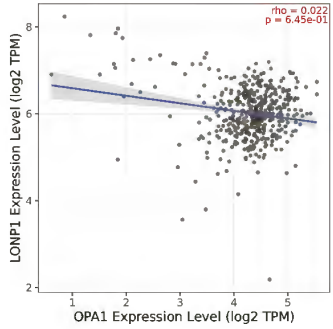
rho = 0.022
p = 6.45e-01
LONP1 Expression Level (log2 TPM)
OPA1 Expression Level (log2 TPM)

B

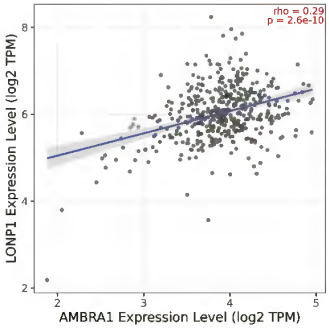
rho = 0.29
p = 2.6e-10
LONP1 Expression Level (log2 TPM)
AMBRA1 Expression Level (log2 TPM)

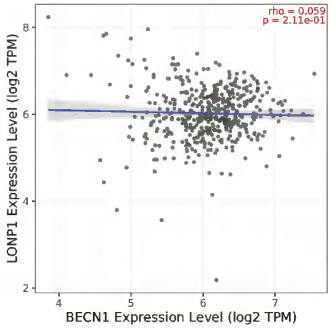
rho = 0.059
p = 2.11e-01
LONP1 Expression Level (log2 TPM)
BECN1 Expression Level (log2 TPM)

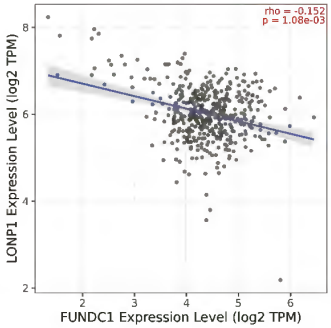
rho = -0.152
p = 1.08e-03
LONP1 Expression Level (log2 TPM)
FUNDC1 Expression Level (log2 TPM)

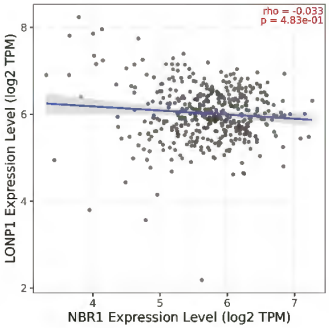
rho = -0.033
p = 4.83e-01
LONP1 Expression Level (log2 TPM)
NBR1 Expression Level (log2 TPM)

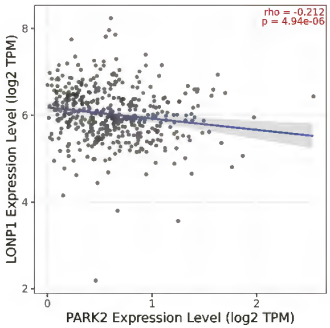
rho = -0.212
p = 4.94e-06
LONP1 Expression Level (log2 TPM)
PARK2 Expression Level (log2 TPM)

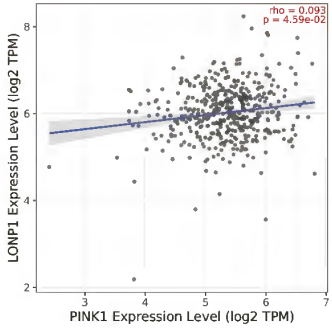
rho = 0.093
p = 4.59e-02
LONP1 Expression Level (log2 TPM)
PINK1 Expression Level (log2 TPM)

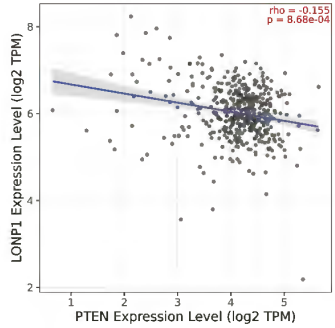
rho = -0.155
p = 8.68e-04
LONP1 Expression Level (log2 TPM)
PTEN Expression Level (log2 TPM)

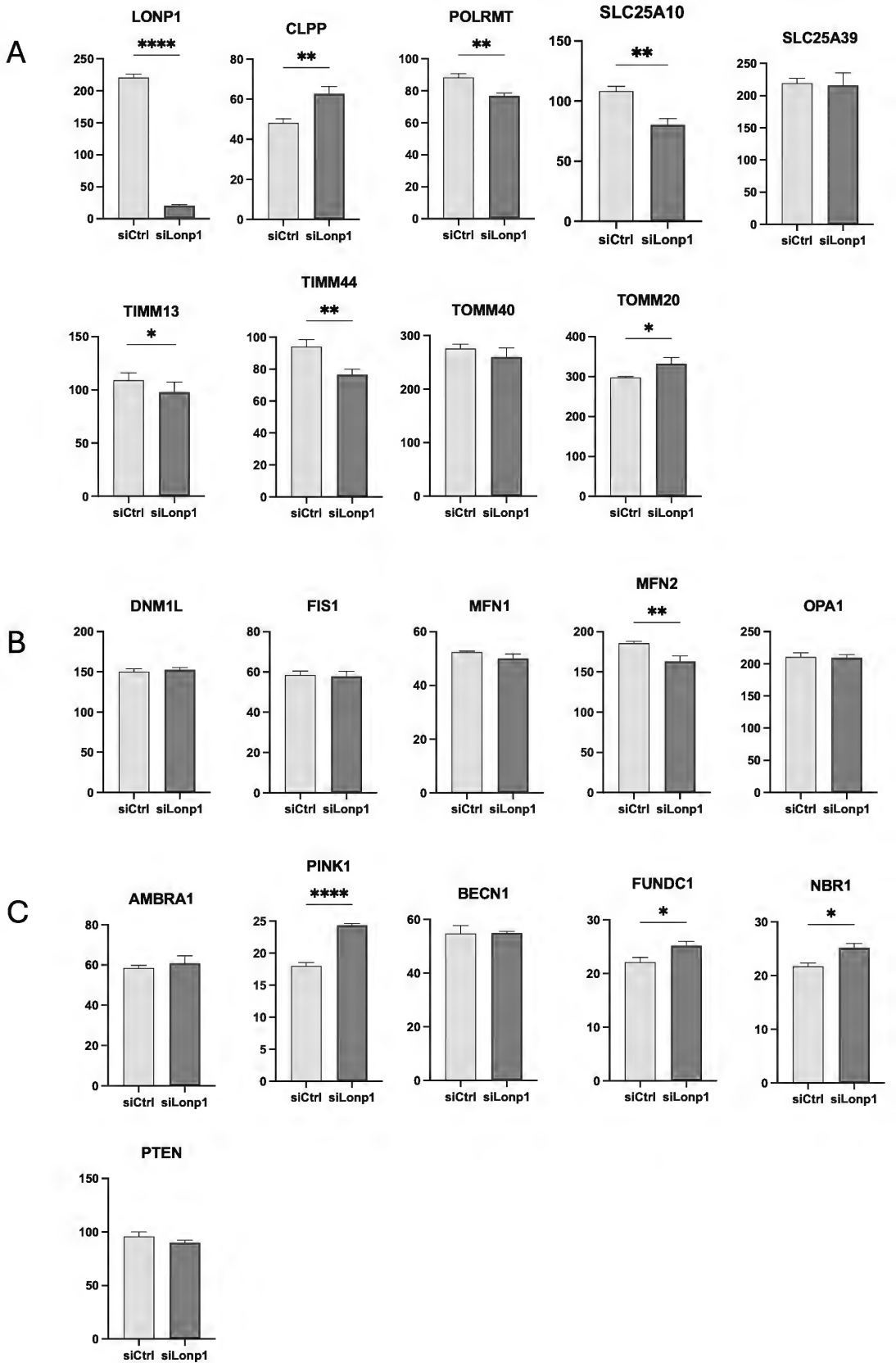
A
LONP1
****
CLPP
**
POLRMT
**
SLC25A10
**
SLC25A39
TIMM13
*
TIMM44
**
TOMM40
TOMM20
*
siCtrl siLonp1
B
DNM1L
FIS1
MFN1
MFN2
**
OPA1
C
AMBRA1
PINK1
****
BECN1
FUNDC1
*
NBR1
*
PTEN

A

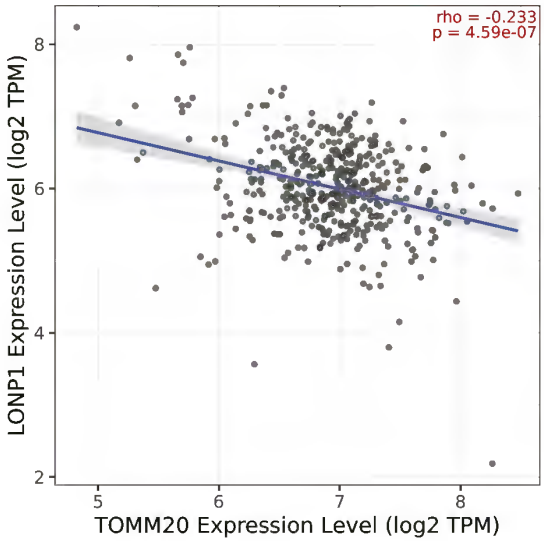
rho = -0.233
p = 4.59e-07
LONP1 Expression Level (log2 TPM)
TOMM20 Expression Level (log2 TPM)
2
4
6
8
5
6
7
8

B

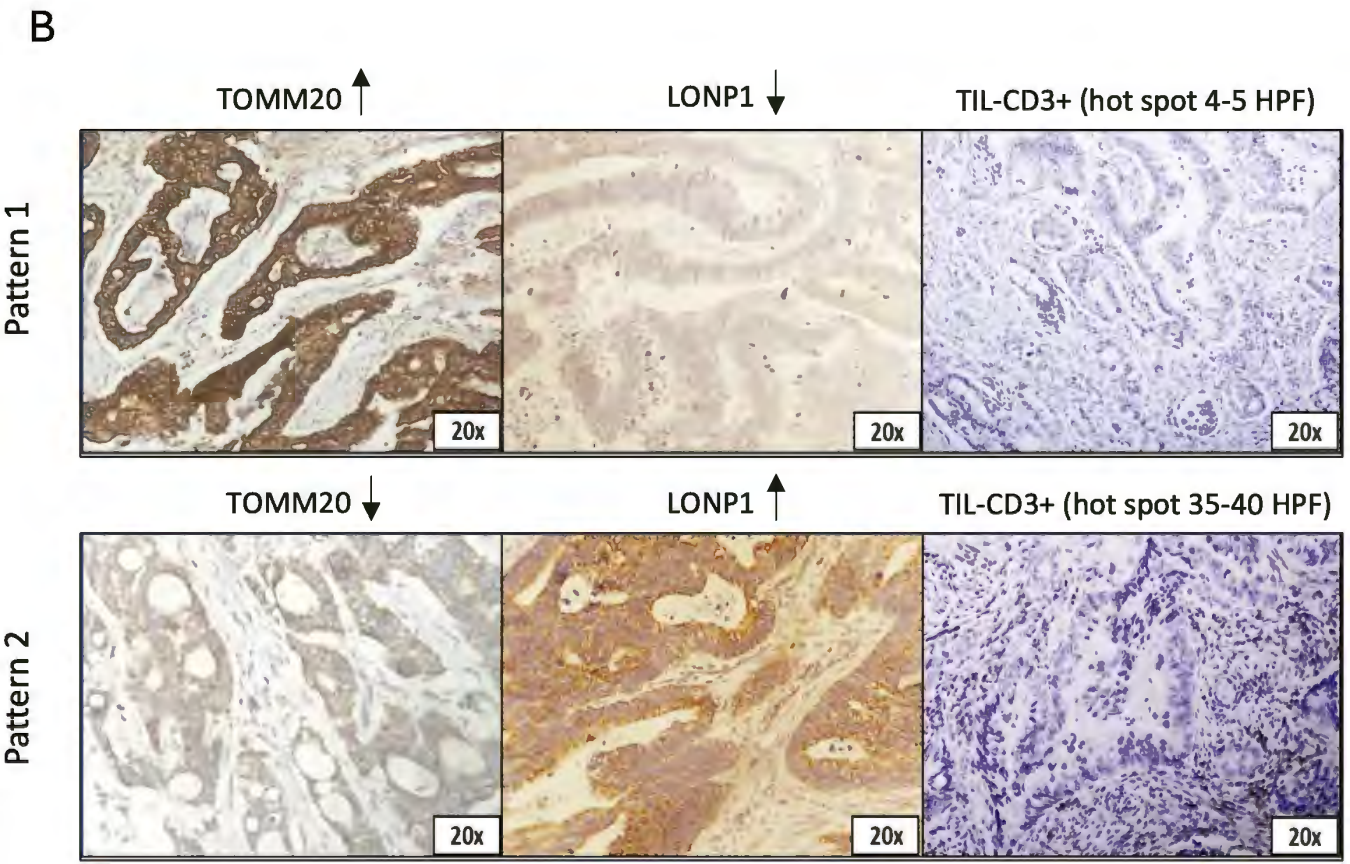
TOMM20
LONP1
TIL-CD3+ (hot spot 4-5 HPF)
Pattern 1
20x
20x
20x
TOMM20
LONP1
TIL-CD3+ (hot spot 35-40 HPF)
Pattern 2
20x
20x
20x

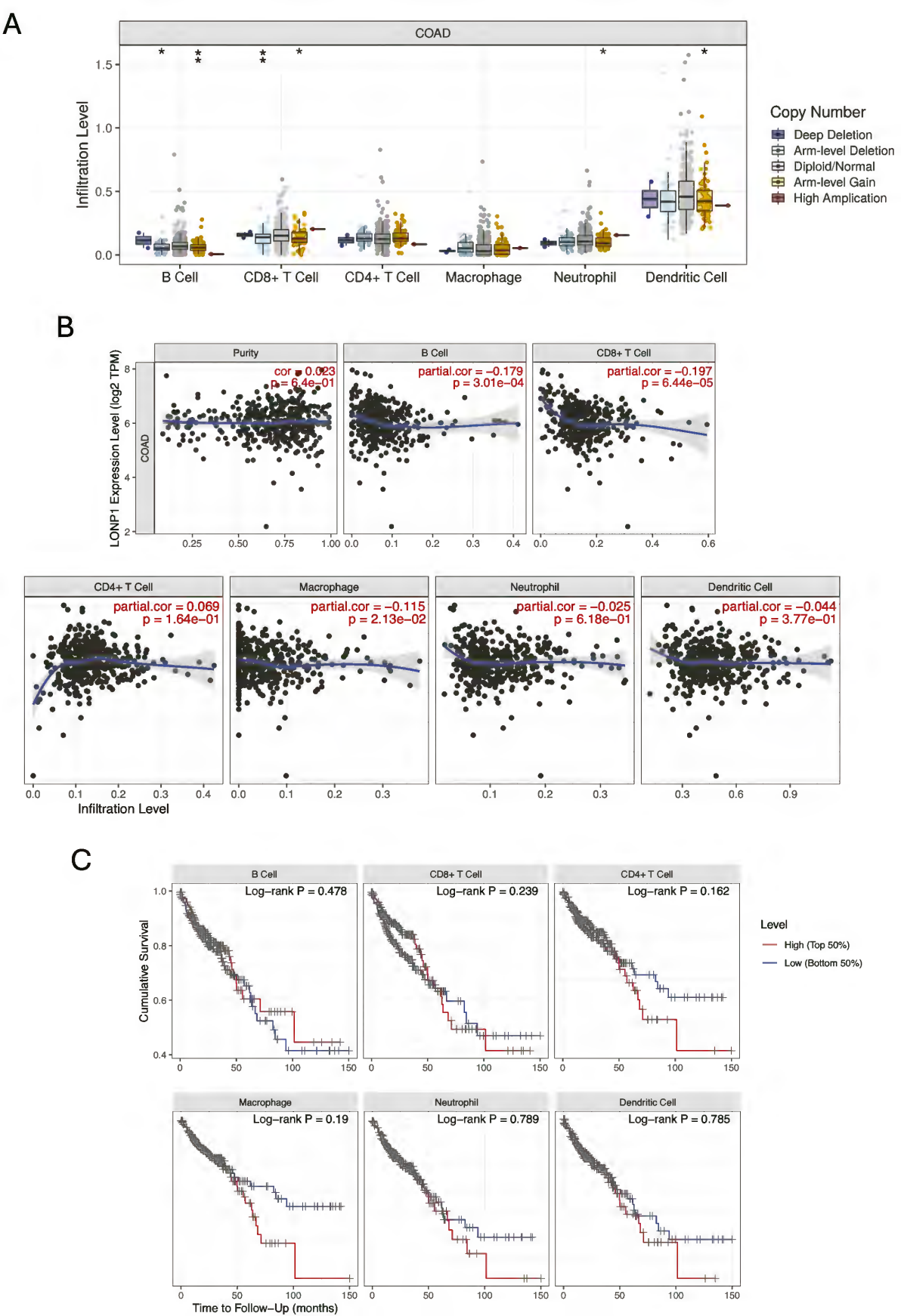
A
COAD
Infiltration Level
1.5
1.0
0.5
0.0
B Cell
CD8+ T Cell
CD4+ T Cell
Macrophage
Neutrophil
Dendritic Cell
Copy Number
Deep Deletion
Arm-level Deletion
Diploid/Normal
Arm-level Gain
High Amplication
B
LONP1 Expression Level (log2 TPM)
COAD
Purity
cor = 0.023
p = 6.4e−01
B Cell
partial.cor = −0.179
p = 3.01e−04
CD8+ T Cell
partial.cor = −0.197
p = 6.44e−05
CD4+ T Cell
partial.cor = 0.069
p = 1.64e−01
Macrophage
partial.cor = −0.115
p = 2.13e−02
Neutrophil
partial.cor = −0.025
p = 6.18e−01
Dendritic Cell
partial.cor = −0.044
p = 3.77e−01
Infiltration Level
C
B Cell
Log−rank P = 0.478
CD8+ T Cell
Log−rank P = 0.239
CD4+ T Cell
Log−rank P = 0.162
Cumulative Survival
Level
High (Top 50%)
Low (Bottom 50%)
Macrophage
Log−rank P = 0.19
Neutrophil
Log−rank P = 0.789
Dendritic Cell
Log−rank P = 0.785
Time to Follow−Up (months)

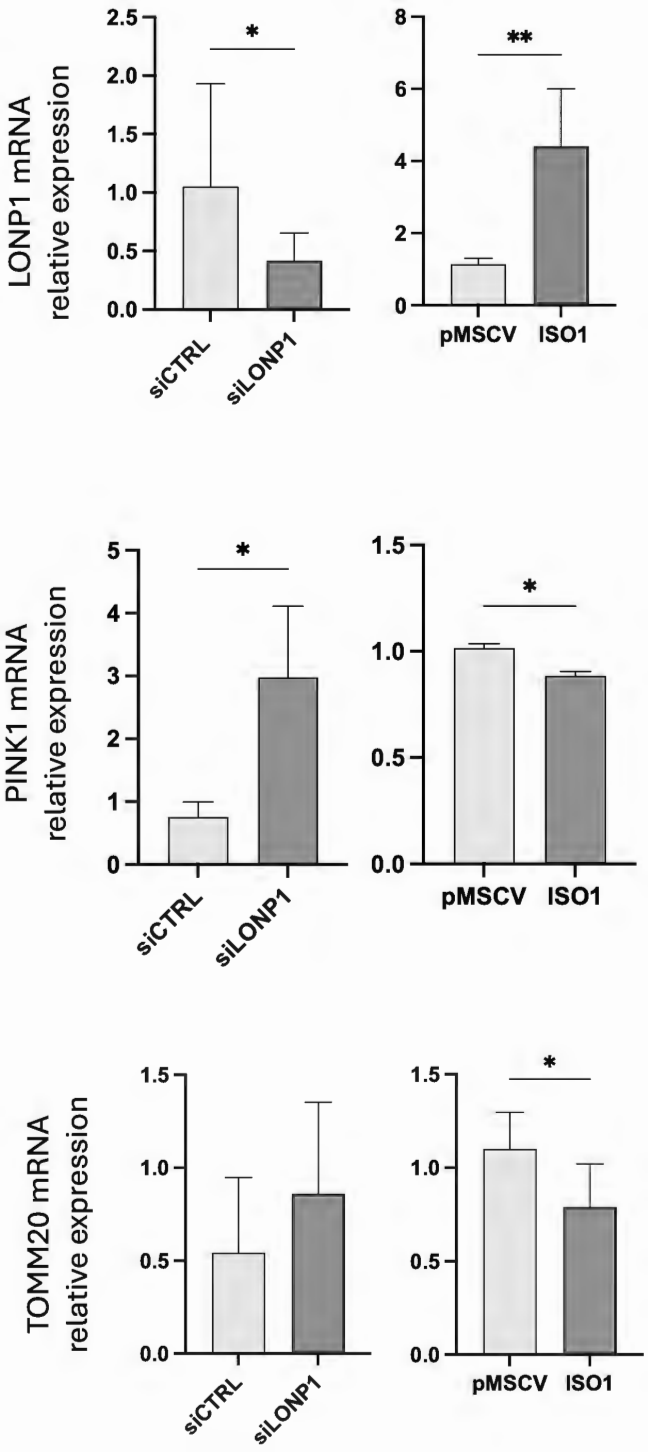
LONP1 mRNA
relative expression
2.5
2.0
1.5
1.0
0.5
0.0
*
siCTRL
siLONP1
8
6
4
2
0
**
pMSCV
ISO1
PINK1 mRNA
relative expression
5
4
3
2
1
0
*
siCTRL
siLONP1
1.5
1.0
0.5
0.0
*
pMSCV
ISO1
TOMM20 mRNA
relative expression
1.5
1.0
0.5
0.0
siCTRL
siLONP1
1.5
1.0
0.5
0.0
*
pMSCV
ISO1

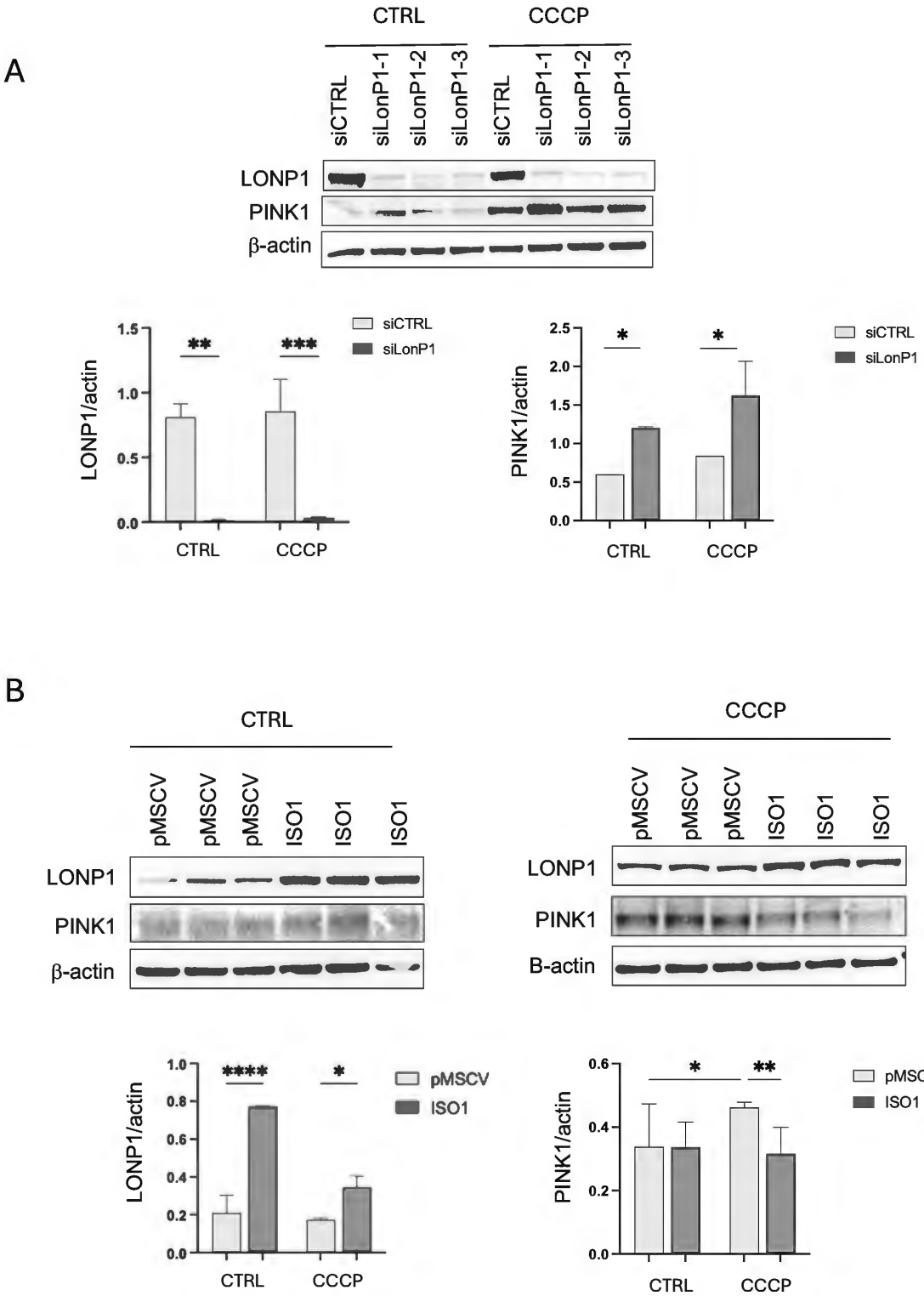
A
CTRL
CCCP
siCTRL
siLonP1-1
siLonP1-2
siLonP1-3
siCTRL
siLonP1-1
siLonP1-2
siLonP1-3
LONP1
PINK1
β-actin
LONP1/actin
1.5
1.0
0.5
0.0
**
***
siCTRL
siLonP1
CTRL
CCCP
PINK1/actin
2.5
2.0
1.5
1.0
0.5
0.0
*
*
siCTRL
siLonP1
CTRL
CCCP
B
CTRL
CCCP
pMSCV
pMSCV
pMSCV
ISO1
ISO1
ISO1
LONP1
PINK1
β-actin
B-actin
LONP1/actin
1.0
0.8
0.6
0.4
0.2
0.0
****
*
pMSCV
ISO1
CTRL
CCCP
PINK1/actin
0.6
0.4
0.2
0.0
*
**
pMSCV
ISO1
CTRL
CCCP

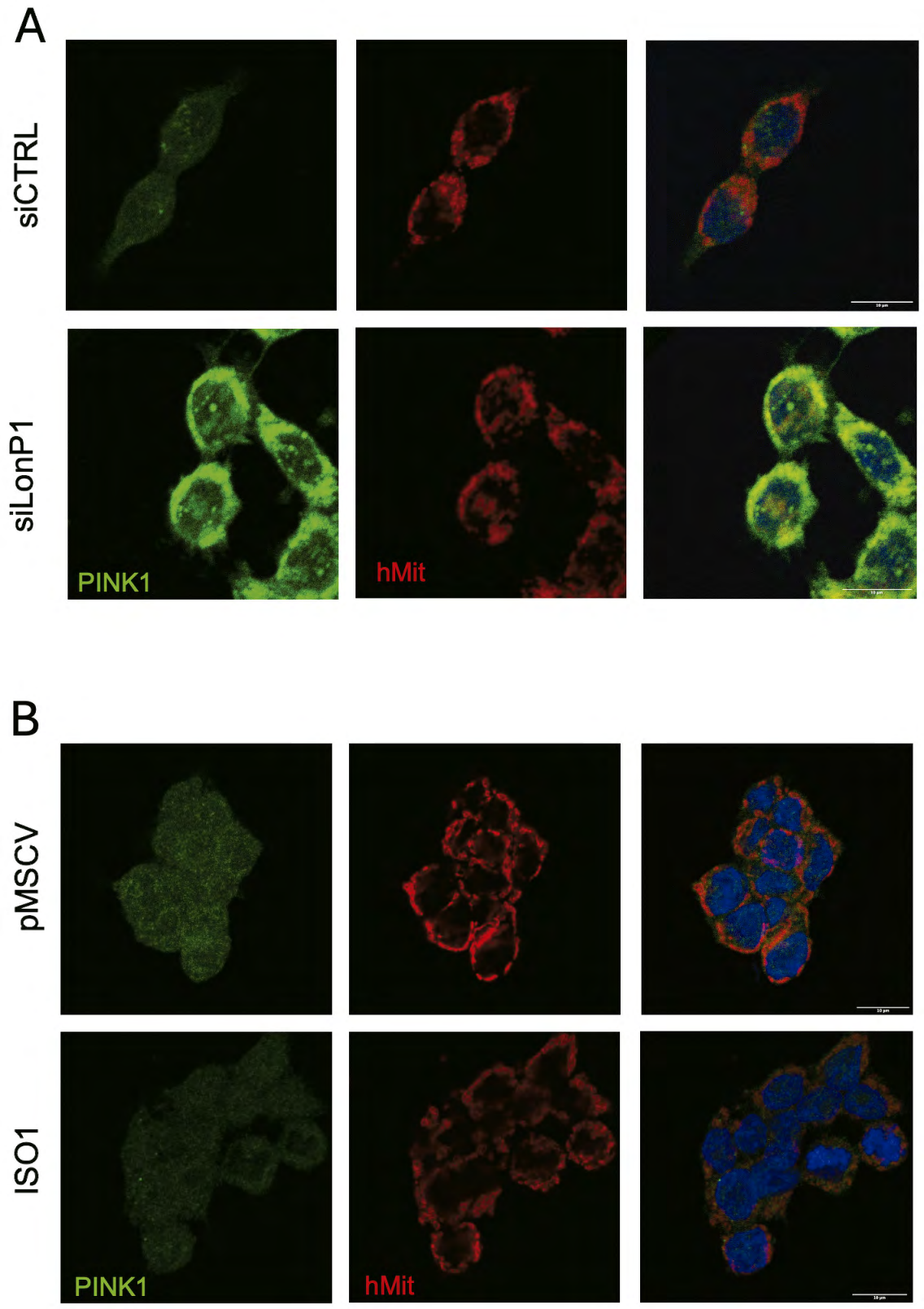
A
siCTRL
siLonP1
PINK1
hMit
B
pMSCV
ISO1
PINK1
hMit